

Physics-preserving enriched Galerkin method for a fully-coupled thermo-poroelasticity model

Son-Young Yi^{1†} and Sanghyun Lee^{2*}

¹Department of Mathematical Sciences, University of Texas at El Paso, 500 W University Ave, El Paso, TX 79968, USA.

²Department of Mathematics, Florida State University, 1017 Academic Way, Tallahassee, FL 32304, USA.

*Corresponding author(s). E-mail(s): lee@math.fsu.edu;

Contributing authors: syi@utep.edu;

†This author contributed equally to this work.

Abstract

This paper proposes a new numerical method for a fully-coupled, quasi-static thermo-poroelasticity model in a unified enriched Galerkin (EG) method framework. In our method, the mechanics sub-problem is solved using a locking-free EG method, and the flow and heat sub-problems are solved using a locally-conservative EG method. The proposed method offers mass and energy conservation properties with much lower costs than other methods with the same properties, including discontinuous Galerkin methods and mixed finite element methods. The well-posedness and optimal a priori error estimates are carefully derived. Several numerical tests confirm the theoretical optimal convergence rates and the mass and energy conservation properties of the new method.

Keywords: Enriched Galerkin, thermo-poroelasticity, mass-conservation, energy-conservation

1 Introduction

Thermal-hydraulic-mechanical (THM) processes refer to a complex interplay of heat transfer, fluid flow, and mechanical responses in natural and engineered porous media. Modeling THM systems has been a subject of great interest in various disciplines, including petroleum engineering, geothermal energy production, and biomedical engineering. One of the widely used mathematical models to describe the THM processes is based on Biot's non-isothermal consolidation theory [1], known as the thermo-poroelasticity model. This model is an extension of the well-known Biot's poroelasticity model [2], which describes the interaction of a deformable porous medium with the fluid flow inside the medium under the iso-thermal condition. The governing equations of the thermo-poroelasticity model have three primary variables: the displacement of the solid, fluid pressure, and temperature, and they consist of the momentum, mass, and energy balance equations. The resulting system of partial differential equations (PDEs) is fully coupled and nonlinear. In this paper, we consider a fully coupled, linear thermo-poroelasticity model, where the energy balance equation is linearized for simplicity but still retains coupling terms with the momentum and mass balance equations.

The complex nature of the thermo-poroelasticity model poses extreme challenges to developing and analyzing numerical schemes. In general, any desirable numerical methods for the thermo-poroelasticity model should preserve the underlying physical laws, such as mass and energy conservation, and be robust with respect to physical and simulation parameters. There have been various numerical methods utilized to solve THM models in the past [3], including finite volume [4, 5], finite difference [6], continuous Galerkin (CG) [7–9], discontinuous Galerkin (DG) [10], and boundary element [11] methods. While some methods utilize the same type of numerical solvers for the entire system (e.g., CG [9] and mixed finite element method [12]), most numerical solvers combine different types of numerical methods tailored for each of the momentum, mass, and energy equations. This is mainly because the three balance equations are different types of PDEs; hence they should be handled differently. However, combining different types of numerical solvers for the coupled system may require special care for the sub-solvers to communicate seamlessly with each other when transferring the solution data. Moreover, a rigorous numerical analysis for such methods is arduous to conduct. This explains the lack of literature dedicated to the mathematical analysis of the numerical solvers of THM models.

The main objective of this paper is to design and analyze a physics-preserving and computationally efficient numerical method to study the thermo-poroelasticity model in a unified numerical framework. Our method is based on the enriched Galerkin (EG) methods. The EG method is a new class of finite element methods that combines the advantages of the CG and DG methods. Its computational costs are much lower than those of the DG method due to the fewer degrees of freedom, leading to a simpler sparse linear system. Moreover, the EG method inherits desirable properties from the

DG method, such as local mass conservation and flexibility with discontinuous coefficients, which the CG method lacks. The original EG method [13], which will be called the locally-conservative EG (LC-EG) method, was developed to study a second-order elliptic problem and has been used for studying coupled flow and transport phenomena in porous media [14–17]. Later, the authors developed a new type of EG method, to be called the locking-free EG (LF-EG) method, to simulate incompressible elastic materials [18]. Since then, this new LF-EG method has been applied to the Stokes flow [19] and poroelasticity model [20]. The new method we propose here utilizes both LC-EG and LF-EG methods to solve the thermo-poroelasticity system. This coupled EG method preserves the underlying physical law for each sub-system, such as mass and energy conservation and incompressibility, at a lower computational cost than other methods with similar capabilities, for instance, a mixed finite element method [12]. We conduct a convergence analysis for the fully-coupled, fully-discrete EG method to prove optimal-order error estimates.

The outline of the rest of this paper is as follows. Section 2 describes the governing equations, followed by the description of the variational problem in Section 3. In Section 4, we define our coupled EG method and discuss its well-posedness and mass and energy conservation properties. Then, Section 5 is dedicated to establishing optimal-order error estimates. Section ?? briefly remarks on extending our EG method for the case of a very large Lamé constant λ . Finally, we provide some numerical results in Section 6.

2 Governing Equations

Let Ω be a bounded, convex, and Lipschitz domain in \mathbb{R}^d , $d = 2, 3$, with the boundary $\partial\Omega$ and let $\mathbb{I} = (0, T]$ with $T > 0$. Then, let $\mathbf{u} : \Omega \times \mathbb{I} \rightarrow \mathbb{R}^d$ be the vector-valued displacement of the solid, $p : \Omega \times \mathbb{I} \rightarrow \mathbb{R}$ the scalar-valued fluid pressure, and $\theta : \Omega \times \mathbb{I} \rightarrow \mathbb{R}$ the scalar-valued temperature. Then, governing equations for thermo-poroelasticity are derived by coupling momentum balance for mechanics based on linear elasticity, mass balance for the pressure, and energy balance for the temperature as follows:

$$-\nabla \cdot (\boldsymbol{\sigma}(\mathbf{u}) - \alpha p \mathbf{I} - 3\alpha_T K_{dr} \theta \mathbf{I}) = \mathbf{f} \quad \text{in } \Omega \times \mathbb{I}, \quad (1a)$$

$$\frac{\partial}{\partial t} (c_0 p + \alpha \nabla \cdot \mathbf{u} - 3\alpha_m \theta) - \nabla \cdot (\mathbf{K} \nabla p) = g \quad \text{in } \Omega \times \mathbb{I}, \quad (1b)$$

$$\frac{\partial}{\partial t} (C_d \theta + 3\alpha_T K_{dr} \theta_0 \nabla \cdot \mathbf{u} - 3\alpha_m \theta_0 p) - \nabla \cdot (\mathbf{D} \nabla \theta) = \eta \quad \text{in } \Omega \times \mathbb{I}, \quad (1c)$$

In the momentum balance equation (1a), $\boldsymbol{\sigma}(\mathbf{u})$ is the standard stress tensor from linear elasticity. It satisfies the constitutive equation $\boldsymbol{\sigma}(\mathbf{u}) := 2\mu\boldsymbol{\epsilon}(\mathbf{u}) + \lambda(\nabla \cdot \mathbf{u})\mathbf{I}$, where $\boldsymbol{\epsilon}(\mathbf{u}) := \frac{1}{2}[\nabla \mathbf{u} + (\nabla \mathbf{u})^T]$ is the strain tensor, \mathbf{I} is the $d \times d$ identity tensor, and μ, λ are the Lamé constants. The Lamé constants are assumed to be in the range $\mu \in [\mu_0, \mu_1]$ and $\lambda \in [0, \infty)$ for some $0 < \mu_0 < \mu_1 < \infty$. Also, \mathbf{f} is the body force, α is the *Biot-Willis* constant, $K_{dr} := (3\lambda + 2\mu)/3$ is the drained isothermal bulk modulus, and α_T is the volumetric skeleton

4 *EG for thermo-poroelasticity*

thermal dilation coefficient. The total stress tensor is given by $\tilde{\sigma}(\mathbf{u}, p, \theta) = \boldsymbol{\sigma}(\mathbf{u}) - \alpha p \mathbf{I} - 3\alpha_T K_{dr} \theta \mathbf{I}$.

The second equation (1b) is the mass balance equation for the fluid, assuming the Darcy law for the volumetric fluid flux: $\mathbf{q} = -\mathbf{K} \nabla p$. We ignore the gravity effect and set the fluid viscosity to be one here for a simple presentation of the numerical method. However, including the gravity term and the fluid viscosity in the numerical formulation is straightforward. Here, $\mathbf{K} \in \mathbb{R}^{d \times d}$ is the permeability tensor, which is symmetric and uniformly positive-definite and satisfies the following assumption: there exist positive constants k_{\min}, k_{\max} such that for any $\mathbf{x} \in \Omega$,

$$k_{\min} \boldsymbol{\xi}^T \boldsymbol{\xi} \leq \boldsymbol{\xi}^T \mathbf{K}(\mathbf{x}) \boldsymbol{\xi} \leq k_{\max} \boldsymbol{\xi}^T \boldsymbol{\xi}, \quad \forall \boldsymbol{\xi} \in \mathbb{R}^d. \quad (2)$$

In addition, $c_0 = 1/M$, where M is Biot's modulus, $3\alpha_m$ is the thermal dilation coefficient, and g is the volumetric fluid source/sink term.

Finally, the energy balance equation, or the heat transfer equation (1c), is obtained by assuming local thermal equilibrium between solid and fluid in pores. Therefore, this energy balance equation is expressed in terms of a single temperature variable θ with the effective total heat conductivity C_d . Also, η is the volumetric heat source/sink term and θ_0 is a reference temperature and is assumed to be nonzero. The use of this reference temperature in the heat equation is justified due to small magnitudes of α_T and α_m [21, 22]. In addition, the bulk thermal conductivity tensor \mathbf{D} , which is symmetric and uniformly positive-definite and assumed to satisfy the following: there exist positive constants d_{\min}, d_{\max} such that for any $\mathbf{x} \in \Omega$,

$$d_{\min} \boldsymbol{\xi}^T \boldsymbol{\xi} \leq \boldsymbol{\xi}^T \mathbf{D}(\mathbf{x}) \boldsymbol{\xi} \leq d_{\max} \boldsymbol{\xi}^T \boldsymbol{\xi}, \quad \forall \boldsymbol{\xi} \in \mathbb{R}^d. \quad (3)$$

To complete the system of governing equations (1), we have to provide initial conditions and boundary conditions. To this end, consider three partitions $\{\Gamma_d, \Gamma_t\}$, $\{\Gamma_p, \Gamma_f\}$, and $\{\Gamma_r, \Gamma_h\}$ of $\partial\Omega$ such that

$$\partial\Omega = \overline{\Gamma_d} \cup \overline{\Gamma_t} = \overline{\Gamma_p} \cup \overline{\Gamma_f} = \overline{\Gamma_r} \cup \overline{\Gamma_h}.$$

Then, the boundary conditions are given as

$$\mathbf{u} = \mathbf{u}_D \text{ on } \Gamma_d, \quad \tilde{\sigma} \mathbf{n} = \mathbf{t}_N \text{ on } \Gamma_t, \quad (4a)$$

$$p = p_D \text{ on } \Gamma_p, \quad \mathbf{K} \nabla p \cdot \mathbf{n} = q_N \text{ on } \Gamma_f, \quad (4b)$$

$$\theta = \theta_D \text{ on } \Gamma_r, \quad \mathbf{D} \nabla \theta \cdot \mathbf{n} = s_N \text{ on } \Gamma_h, \quad (4c)$$

where \mathbf{n} is the outward unit normal vector to $\partial\Omega$. On the other hand, the initial conditions are given as

$$\mathbf{u}(\cdot, 0) = \mathbf{u}^0, \quad p(\cdot, 0) = p^0, \quad \theta(\cdot, 0) = \theta^0 \quad \forall x \in \Omega. \quad (5)$$

These initial conditions must themselves satisfy some constraints, such as the equilibrium equation and the compatibility equation. If the initial conditions are in an equilibrated state, namely satisfying the governing equations in a steady state, they can simply be ignored as we need only to solve the perturbed state.

3 Variational Formulation

In this section, we derive a variational formulation for the model problem (1) and propose a fully-discrete EG method. The standard notation for the L^2 - and Sobolev spaces and their associated inner products and norms will be used here. Also, for any subset Γ of $\partial\Omega$, $H_0^m(\Omega) = \{v \in H^m(\Omega) \mid v = 0 \text{ on } \Gamma\}$.

In order to derive a variational problem, we multiply (1a), (1b), and (1c) by $\mathbf{v} \in [H_{0,\Gamma_d}^1(\Omega)]^d$, $w \in H_{0,\Gamma_p}^1(\Omega)$, and $s \in H_{0,\Gamma_r}^1(\Omega)$, respectively, and integrate by parts. Then, the resulting variational formulation reads as follows: At every time $t \in (0, T]$, find $(\mathbf{u}(\cdot, t), p(\cdot, t), \theta(\cdot, t)) \in [H^1(\Omega)]^d \times H^1(\Omega) \times H^1(\Omega)$ such that $\mathbf{u} = \mathbf{u}_D$ on Γ_d , $p = p_D$ on Γ_p , and $\theta = \theta_D$ on Γ_r and satisfy, for all $(\mathbf{v}, w, s) \in [H_{0,\Gamma_d}^1(\Omega)]^d \times H_{0,\Gamma_p}^1(\Omega) \times H_{0,\Gamma_r}^1(\Omega)$,

$$\mathbf{a}^{\mathbf{u}}(\mathbf{u}, \mathbf{v}) - \alpha(p, \nabla \cdot \mathbf{v}) - 3\alpha_T K_{dr}(\theta, \nabla \cdot \mathbf{v}) = (\mathbf{f}, \mathbf{v}) + (\mathbf{t}_N, \mathbf{v})_{\Gamma_t}, \quad (6a)$$

$$c_0(p_t, w) + \alpha(\nabla \cdot \mathbf{u}_t, w) - 3\alpha_m(\theta_t, w) + \mathbf{a}^p(p, w) = (g, w) + (q_N, w)_{\Gamma_f}, \quad (6b)$$

$$C_d(\theta_t, s) + 3\alpha_T K_{dr}\theta_0(\nabla \cdot \mathbf{u}_t, s) - 3\alpha_m\theta_0(p_t, s) + \mathbf{a}^\theta(\theta, s) = (\eta, s) + (s_N, s)_{\Gamma_h}, \quad (6c)$$

where the bilinear forms $\mathbf{a}^{\mathbf{u}}(\cdot, \cdot)$, $\mathbf{a}^p(\cdot, \cdot)$, and $\mathbf{a}^\theta(\cdot, \cdot)$ are defined by

$$\begin{aligned} \mathbf{a}^{\mathbf{u}}(\mathbf{u}, \mathbf{v}) &:= 2\mu(\varepsilon(\mathbf{u}), \varepsilon(\mathbf{v})) + \lambda(\nabla \cdot \mathbf{u}, \nabla \cdot \mathbf{v}) & \forall \mathbf{u}, \mathbf{v} \in [H^1(\Omega)]^d, \\ \mathbf{a}^p(p, w) &:= (\mathbf{K}\nabla p, \nabla w) & \forall p, w \in H^1(\Omega), \\ \mathbf{a}^\theta(\theta, s) &:= (\mathbf{D}\nabla\theta, \nabla s) & \forall \theta, s \in H^1(\Omega). \end{aligned}$$

The well-posedness of the same variational problem as (6) except for an extra nonlinear coupling term $-\mathbf{K}\nabla p \cdot \nabla\theta$ in the temperature equation (6c) was studied in [9], where they studied the standard CG method for the model.

4 Discretization by Enriched Galerkin Method

Let $\mathcal{T}_h = \{K\}$ be a shape-regular triangulation of the domain Ω into triangular or rectangular elements with a mesh size $h = \max_K h_K$, where h_K is the diameter of $K \in \mathcal{T}_h$. We denote by \mathcal{E}_h the set of all edges in the mesh and by \mathcal{E}_h^I the set of all the interior edges. For each $K \in \mathcal{T}_h$, denote the boundary of K by ∂K and the outward unit normal vector to ∂K by \mathbf{n}_K . If $e \in \mathcal{E}_h^I$, we assign to e a fixed unit normal vector \mathbf{n}_e .

6 *EG for thermo-poroelasticity*

The EG formulation requires jump and average operators. First, let us define the following broken Sobolev subspace on \mathcal{T}_h : For any real number $s > 0$,

$$H^s(\mathcal{T}_h) = \{w \in L^2(\Omega) \mid w|_K \in H^s(K), K \in \mathcal{T}_h\},$$

equipped with a broken inner product $(w, q)_{\mathcal{T}_h} = \sum_{K \in \mathcal{T}_h} (w, q)_K$. Then, for any function $w \in H^s(\mathcal{T}_h)$ with $s > 1/2$ and $e \in \mathcal{E}_h^I$, let

$$[w] = w^+ - w^- \quad \text{and} \quad \{w\} = \frac{1}{2}(w^+ + w^-),$$

where $w^\pm = (w|_{K^\pm})|_e$. Here, K^\pm are the two neighboring elements of e . If $e \in \partial\Omega$, then e belongs to only one triangle K , and we define

$$[w] = \{w\} = (w|_K)|_e.$$

The above definitions of the broken Sobolev space and jump and average operators can be naturally extended to vector-valued functions. We will use the same notations in that case.

For the spatial discretization of the weak form (6) by our EG method, let us introduce our LF-EG space [18] for the displacement and LC-EG space [14, 16] for the pressure and temperature on \mathcal{T}_h . First, let $\mathbb{P}_k(E)$ be the space of all polynomials of degree at most $k \geq 0$ on a set E and $\mathbb{Q}_k(E)$ be the space of all polynomials on a set E that are of degree $\leq k$ in each of the variables x_i for $i = 1, \dots, d$. We then let \mathbb{P}_1^{CG} and \mathbb{Q}_1^{CG} be the standard linear and bilinear CG finite element spaces on triangular and quadrilateral meshes. That is,

$$\begin{aligned} \mathbb{P}_1^{CG} &:= \{\psi \in H^1(\Omega) \mid \psi|_K \in \mathbb{P}_1(K) \quad \forall K \in \mathcal{T}_h\}, \\ \mathbb{Q}_1^{CG} &:= \{\psi \in H^1(\Omega) \mid \psi|_K \in \mathbb{Q}_1(K) \quad \forall K \in \mathcal{T}_h\}. \end{aligned}$$

We use a notation \mathbb{C}_1^{CG} for \mathbb{P}_1^{CG} on a triangular mesh and \mathbb{Q}_1^{CG} on a quadrilateral mesh.

To define the LF-EG space, we need the following discontinuous space:

$$\mathbb{D}_1^{DG} = \{\psi \in [L^2(\Omega)]^d \mid \psi|_K = c_K(\mathbf{x} - \mathbf{x}_K), \quad c_K \in \mathbb{R} \quad \forall K \in \mathcal{T}_h\},$$

where $\mathbf{x} = [x_1, \dots, x_d]^T$ and \mathbf{x}_K is the center of $K \in \mathcal{T}_h$. Then, the LF-EG space for the displacement is constructed by enriching the vector-valued CG space, $[\mathbb{C}_1^{CG}]^d$, by this space \mathbb{D}_1^{DG} . That is,

$$\mathbf{V}_h := [\mathbb{C}_1^{CG}]^d \oplus \mathbb{D}_1^{DG},$$

in which the direct sum above is true because $[\mathbb{C}_1^{CG}]^d \cap \mathbb{D}_1^{DG}$ contains only the zero constant function.

To define the LC-EG space for the pressure and temperature, let \mathbb{P}_0^{DG} be the piecewise constant space on \mathcal{T}_h :

$$\mathbb{P}_0^{DG} = \{\psi \in L^2(\Omega) \mid \psi|_K \in \mathbb{P}_0(K) \quad \forall K \in \mathcal{T}_h\}.$$

Then, the LC-EG space is defined as

$$\mathcal{W}_h := \mathbb{C}_1^{CG} + \mathbb{P}_0^{DG}.$$

Both \mathcal{V}_h and \mathcal{W}_h require only one additional local degree of freedom per element compared to the linear CG spaces regardless of the dimension d .

These EG spaces are equipped with the following energy norms:

$$\begin{aligned} \|\mathbf{v}\|_{\mathcal{V}} &= (\|\boldsymbol{\epsilon}(\mathbf{v})\|_{0,\mathcal{T}_h}^2 + \beta^{\mathbf{u}} h_e^{-1} \|\llbracket \mathbf{v} \rrbracket\|_{0,\mathcal{E}_h}^2)^{\frac{1}{2}} \quad \forall \mathbf{v} \in \mathcal{V}_h, \\ \|w\|_{\mathcal{W}} &= (\|\nabla w\|_{0,\mathcal{T}_h}^2 + \beta^p h_e^{-1} \|\llbracket w \rrbracket\|_{0,\mathcal{E}_h}^2)^{\frac{1}{2}} \quad \forall w \in \mathcal{W}_h. \end{aligned}$$

The penalty parameter β^p in the norm $\|\cdot\|_{\mathcal{W}}$ can be replaced by β^θ . Indeed, we use the same value for β^p and β^θ in all of our numerical experiments to be presented in Section 6.

To discretize (6) in time, we employ the backward Euler method for simplicity. However, higher-order time-stepping methods can also be considered in practice to achieve the same convergence orders in space and time. For a positive integer N , $\Delta t = T/N$ is the time step and $t^n = n\Delta t$. For any known function $\phi(t)$, the function value at time t^n is denoted by ϕ^n . That is, $\phi^n = \phi(t^n)$. In our EG method, $(\mathbf{u}_h^n, p_h^n, \theta_h^n)$ is an approximation of $(\mathbf{u}^n, p^n, \theta^n)$, where $n = 0, \dots, N$. We use the following notation for the backward difference formula of a time derivative of both vector-valued and scalar-valued functions:

$$D_t \phi^{n+1} = \frac{\phi^{n+1} - \phi^n}{\Delta t}.$$

Finally, our fully-discrete mixed EG method reads as follows: Given $(\mathbf{u}_h^n, p_h^n, \theta_h^n) \in \mathcal{V}_h \times \mathcal{W}_h \times \mathcal{W}_h$ for $0 \leq n \leq N-1$, find $(\mathbf{u}_h^{n+1}, p_h^{n+1}, \theta_h^{n+1}) \in \mathcal{V}_h \times \mathcal{W}_h \times \mathcal{W}_h$ such that

$$\mathbf{a}_h^{\mathbf{u}}(\mathbf{u}_h^{n+1}, \mathbf{v}) - \alpha \mathbf{b}_h(\mathbf{v}, p_h^{n+1}) - 3\alpha_T K_{dr} \mathbf{b}_h(\mathbf{v}, \theta_h^{n+1}) = \mathbf{g}_h^{\mathbf{u}}(t^{n+1}; \mathbf{v}), \quad (7a)$$

$$\begin{aligned} c_0(D_t p_h^{n+1}, w) + \alpha \mathbf{b}_h(D_t \mathbf{u}_h^{n+1}, w) - 3\alpha_m (D_t \theta_h^{n+1}, w) + \mathbf{a}_h^p(p_h^{n+1}, w) \\ = \mathbf{g}_h^p(t^{n+1}; w), \end{aligned} \quad (7b)$$

$$\begin{aligned} C_d(D_t \theta_h^{n+1}, s) + 3\alpha_T K_{dr} \theta_0 \mathbf{b}_h(D_t \mathbf{u}_h^{n+1}, s) - 3\alpha_m \theta_0 (D_t p_h^{n+1}, s) + \mathbf{a}_h^\theta(\theta_h^{n+1}, s) \\ = \mathbf{g}_h^\theta(t^{n+1}; s), \end{aligned} \quad (7c)$$

for $\forall (\mathbf{v}, w, s) \in \mathcal{V}_h \times \mathcal{W}_h \times \mathcal{W}_h$, where the bilinear forms are defined as

$$\mathbf{a}_h^{\mathbf{u}}(\mathbf{w}, \mathbf{v}) := 2\mu(\boldsymbol{\epsilon}(\mathbf{w}), \boldsymbol{\epsilon}(\mathbf{v}))_{\mathcal{T}_h} + \lambda(\nabla \cdot \mathbf{w}, \nabla \cdot \mathbf{v})_{\mathcal{T}_h} - \langle \{\boldsymbol{\sigma}(\mathbf{w}) \mathbf{n}_e\}, \llbracket \mathbf{v} \rrbracket \rangle_{\mathcal{E}_h^I \cup \Gamma_d}$$

$$\begin{aligned}
& - \langle [\![\mathbf{w}]\!], \{\boldsymbol{\sigma}(\mathbf{v})\mathbf{n}_e\} \rangle_{\mathcal{E}_h^I \cup \Gamma_d} + \beta^{\mathbf{u}} \langle h_e^{-1} [\![\mathbf{w}]\!], [\![\mathbf{v}]\!] \rangle_{e \in \mathcal{E}_h^I \cup \Gamma_d}, \\
\mathbf{a}_h^p(q, w) & := (\mathbf{K} \nabla q, \nabla w)_{\mathcal{T}_h} - \langle \{\mathbf{K} \nabla q \cdot \mathbf{n}_e\} [\![w]\!] \rangle_{\mathcal{E}_h^I \cup \Gamma_p} - \langle \{\mathbf{K} \nabla w \cdot \mathbf{n}_e\}, [\![q]\!] \rangle_{\mathcal{E}_h^I \cup \Gamma_p} \\
& \quad + \beta^p \langle h_e^{-1} [\![q]\!], [\![w]\!] \rangle_{\mathcal{E}_h^I \cup \Gamma_p}, \\
\mathbf{a}_h^\theta(q, s) & := (\mathbf{D} \nabla q, \nabla s)_{\mathcal{T}_h} - \langle \{\mathbf{D} \nabla q \cdot \mathbf{n}_e\} [\![s]\!] \rangle_{\mathcal{E}_h^I \cup \Gamma_r} - \langle \{\mathbf{D} \nabla s \cdot \mathbf{n}_e\}, [\![q]\!] \rangle_{\mathcal{E}_h^I \cup \Gamma_r} \\
& \quad + \beta^\theta \langle h_e^{-1} [\![q]\!], [\![s]\!] \rangle_{\mathcal{E}_h^I \cup \Gamma_r}, \\
\mathbf{b}_h(\mathbf{v}, w) & := (\nabla \cdot \mathbf{v}, w)_{\mathcal{T}_h} - \langle \{w\}, [\![\mathbf{v}]\!] \cdot \mathbf{n}_e \rangle_{\mathcal{E}_h^I \cup \Gamma_d},
\end{aligned}$$

and the linear functionals are defined as

$$\begin{aligned}
\mathbf{g}_h^{\mathbf{u}}(t; \mathbf{v}) & := (\mathbf{f}(t), \mathbf{v})_{\mathcal{T}_h} + \langle \mathbf{t}_N(t), \mathbf{v} \rangle_{\Gamma_t} - \langle \mathbf{u}_D(t), \boldsymbol{\sigma}(\mathbf{v})\mathbf{n}_e \rangle_{\Gamma_d} \\
& \quad + \beta^{\mathbf{u}} \langle h_e^{-1} \mathbf{u}_D(t), \mathbf{v} \rangle_{\Gamma_d}, \\
\mathbf{g}_h^p(t; w) & := (g(t), w)_{\mathcal{T}_h} + \langle q_N(t), w \rangle_{\Gamma_f} - \alpha \langle w, (\mathbf{u}_D)_t(t) \cdot \mathbf{n}_e \rangle_{\Gamma_d} \\
& \quad - \langle \mathbf{K} \nabla w \cdot \mathbf{n}_e, p_D(t) \rangle_{\Gamma_p} + \beta^p \langle h_e^{-1} p_D(t), w \rangle_{\Gamma_p}, \\
\mathbf{g}_h^\theta(t; s) & := (\eta(t), s)_{\mathcal{T}_h} + \langle s_N(t), s \rangle_{\Gamma_h} - 3\alpha_T K_{dr} \theta_0 \langle s, (\mathbf{u}_D)_t(t) \cdot \mathbf{n}_e \rangle_{\Gamma_d} \\
& \quad - \langle \mathbf{D} \nabla s \cdot \mathbf{n}_e, \theta_D(t) \rangle_{\Gamma_r} + \beta^\theta \langle h_e^{-1} \theta_D(t), s \rangle_{\Gamma_r},
\end{aligned}$$

where $h_e = |e|^{\frac{1}{d-1}}$ and $|e|$ denotes the length of e in two dimensions and the area in three dimensions. Also, $\beta^{\mathbf{u}} > 0$, $\beta^p > 0$, and $\beta^\theta > 0$ are penalty parameters, which are assumed to be constants in this paper.

4.1 Well-posedness and conservation properties

We start with this subsection with continuity and coercivity lemmas that will be useful for the well-posedness and convergence analysis of the proposed method. The detailed proofs are available in the paper [20] by the authors.

Lemma 4.1 *There exist constants $C_{a_{\mathbf{u}}}, C_{a_p}$, and $C_{a_\theta} > 0$, all independent of h , such that*

$$\mathbf{a}_h^{\mathbf{u}}(\mathbf{v}, \mathbf{w}) \leq C_{a_{\mathbf{u}}} \|\mathbf{v}\|_{\mathcal{V}} \|\mathbf{w}\|_{\mathcal{V}} \quad \forall (\mathbf{v}, \mathbf{w}) \in [H^1(\mathcal{T}_h)]^d \times [H^1(\mathcal{T}_h)]^d, \quad (8a)$$

$$\mathbf{a}_h^p(q, w) \leq C_{a_p} \|q\|_{\mathcal{W}} \|w\|_{\mathcal{W}} \quad \forall (q, w) \in H^1(\mathcal{T}_h) \times H^1(\mathcal{T}_h), \quad (8b)$$

$$\mathbf{a}_h^\theta(q, s) \leq C_{a_\theta} \|q\|_{\mathcal{W}} \|s\|_{\mathcal{W}} \quad \forall (q, s) \in H^1(\mathcal{T}_h) \times H^1(\mathcal{T}_h). \quad (8c)$$

Lemma 4.2 *There exist constants C_b and $C_{\tilde{b}} > 0$, both independent of h , such that*

$$\mathbf{b}_h(\mathbf{v}, w) \leq C_b \|\mathbf{v}\|_{\mathcal{V}} \|w\|_0 \quad \forall (\mathbf{v}, w) \in [H^1(\mathcal{T}_h)]^d \times L^2(\Omega), \quad (9a)$$

$$\mathbf{b}_h(\mathbf{v}, w) \leq C_{\tilde{b}} \|\mathbf{v}\|_0 \|w\|_{\mathcal{W}} \quad \forall (\mathbf{v}, w) \in [H^1(\Omega)]^d \times H^1(\mathcal{T}_h). \quad (9b)$$

Lemma 4.3 *For large enough $\beta^{\mathbf{u}}, \beta^p$, and $\beta^\theta > 0$, the bilinear forms $\mathbf{a}_h^{\mathbf{u}}$, \mathbf{a}_h^p , and \mathbf{a}_h^θ satisfy the following coercivity conditions: there exist $\kappa_{\mathbf{u}}, \kappa_p > 0$, and $\kappa_\theta > 0$, such*

that

$$\kappa_{\mathbf{u}} \|\mathbf{v}\|_{\mathcal{V}}^2 \leq \mathbf{a}_h^{\mathbf{u}}(\mathbf{v}, \mathbf{v}) \quad \forall \mathbf{v} \in \mathcal{V}_h, \quad (10a)$$

$$\kappa_p \|w\|_{\mathcal{W}}^2 \leq \mathbf{a}_h^p(w, w) \quad \forall w \in \mathcal{W}_h, \quad (10b)$$

$$\kappa_{\theta} \|s\|_{\mathcal{W}}^2 \leq \mathbf{a}_h^{\theta}(s, s) \quad \forall s \in \mathcal{W}_h. \quad (10c)$$

Lemma 4.4 *The fully-coupled and fully-discrete EG method (7) for solving the thermo-poroelasticity problem (1) has a unique solution, provided that the penalty parameters $\beta^{\mathbf{u}}$, β^p , and β^{θ} are large enough.*

Proof Given a unique solution from the previous time step n , we want to prove the existence and uniqueness at each time step $n+1$ for $n = 0, \dots, N-1$. Thanks to the finite dimensionality of the solution space, it suffices to prove the uniqueness at each time step. To this end, consider the following homogeneous problem

$$\mathbf{a}_h^{\mathbf{u}}(\mathbf{u}_h^{n+1}, \mathbf{v}) - \alpha \mathbf{b}_h(\mathbf{v}, p_h^{n+1}) - 3\alpha_T K_{dr} \mathbf{b}_h(\mathbf{v}, \theta_h^{n+1}) = 0, \quad (11a)$$

$$c_0(p_h^{n+1}, w) + \alpha \mathbf{b}_h(\mathbf{u}_h^{n+1}, w) - 3\alpha_m(\theta_h^{n+1}, w) + \Delta t \mathbf{a}_h^p(p_h^{n+1}, w) = 0, \quad (11b)$$

$$C_d(\theta_h^{n+1}, s) + 3\alpha_T K_{dr} \theta_0 \mathbf{b}_h(\mathbf{u}_h^{n+1}, s) - 3\alpha_m \theta_0(p_h^{n+1}, s) + \Delta t \mathbf{a}_h^{\theta}(\theta_h^{n+1}, s) = 0 \quad (11c)$$

for $\forall \mathbf{v} \in \mathcal{V}_h$, $\forall w \in \mathcal{W}_h$, and $\forall s \in \mathcal{W}_h$. We wish to prove that the solution to this homogeneous problem is only a trivial solution. Then, take $\mathbf{v} = \theta_0 \mathbf{u}_h^{n+1}$, $w = \theta_0 p_h^{n+1}$, $s = \theta_h^{n+1}$ in (11) to obtain

$$\begin{aligned} \theta_0 \mathbf{a}_h^{\mathbf{u}}(\mathbf{u}_h^{n+1}, \mathbf{u}_h^{n+1}) + c_0 \theta_0(p_h^{n+1}, p_h^{n+1}) + \theta_0 \Delta t \mathbf{a}_h^p(p_h^{n+1}, p_h^{n+1}) \\ + C_d(\theta_h^{n+1}, \theta_h^{n+1}) + \Delta t \mathbf{a}_h^{\theta}(\theta_h^{n+1}, \theta_h^{n+1}) - 6\alpha_m \theta_0(\theta_h^{n+1}, p_h^{n+1}) = 0. \end{aligned}$$

Using the coercivity of the bilinear forms $\mathbf{a}_h^{\mathbf{u}}$, \mathbf{a}_h^p , and \mathbf{a}_h^{θ} in (10) for large enough $\beta^{\mathbf{u}}$, β^p , and β^{θ} and applying the Cauchy-Schwarz and Young's inequalities to the last term, we obtain the following lower bound for the left-hand side of the above equation, which is less than 0 as the right-hand side is equal to 0:

$$\begin{aligned} & \theta_0 \kappa_{\mathbf{u}} \|\mathbf{u}_h^{n+1}\|_{\mathcal{V}}^2 + c_0 \theta_0 \|p_h^{n+1}\|_0^2 + \theta_0 \kappa_p \Delta t \|p_h^{n+1}\|_{\mathcal{W}}^2 \\ & + C_d \|\theta_h^{n+1}\|_0^2 + \kappa_{\theta} \Delta t \|\theta_h^{n+1}\|_{\mathcal{W}}^2 - 3\alpha_m \theta_0 \left(\|\theta_h^{n+1}\|_0^2 + \|p_h^{n+1}\|_0^2 \right) \\ & = \theta_0 \kappa_{\mathbf{u}} \|\mathbf{u}_h^{n+1}\|_{\mathcal{V}}^2 + (c_0 - 3\alpha_m) \theta_0 \|p_h^{n+1}\|_0^2 + \theta_0 \kappa_p \Delta t \|p_h^{n+1}\|_{\mathcal{W}}^2 \\ & + (C_d - 3\alpha_m \theta_0) \|\theta_h^{n+1}\|_0^2 + \kappa_{\theta} \Delta t \|\theta_h^{n+1}\|_{\mathcal{W}}^2 \leq 0. \end{aligned}$$

Therefore,

$$\|\mathbf{u}_h^{n+1}\|_{\mathcal{V}} = \|p_h^{n+1}\|_{\mathcal{W}} = \|\theta_h^{n+1}\|_{\mathcal{W}} = 0,$$

from which we see the homogeneous system (11) has only a trivial solution. \square

We will now show that our EG method conserves mass and energy (or enthalpy) [22] on each mesh element. To see this, let us fix an interior element $K \in \mathcal{T}_h$ and integrate the mass and energy balance equations, (1b) and (1c), by parts over K . If we let $\mathbf{q}_p = -\mathbf{K} \nabla p$ and $\mathbf{q}_{\theta} = -\mathbf{D} \nabla \theta$, we have

$$\langle \mathbf{q}_p \cdot \mathbf{n}_K, 1 \rangle_{\partial K} = (g, 1)_K - c_0(p_t, 1)_K - \alpha \langle \mathbf{u}_t \cdot \mathbf{n}_K, 1 \rangle_{\partial K} + 3\alpha_m(\theta_t, 1)_K, \quad (12a)$$

$$\begin{aligned} \langle \mathbf{q}_\theta \cdot \mathbf{n}_K, 1 \rangle_{\partial K} &= (\eta, 1)_K - C_d(\theta_t, 1)_K - 3\alpha_T K_{dr} \theta_0 \langle \mathbf{u}_t \cdot \mathbf{n}_K, 1 \rangle_{\partial K} \\ &\quad + 3\alpha_m \theta_0 (p_t, 1)_K. \end{aligned} \quad (12b)$$

The above equations, (12a) and (12b), represent the local mass and energy conservation equations satisfied by the true solution p and θ , respectively. The following lemma derives discrete counterparts of these conservation equations satisfied by our EG method.

Lemma 4.5 *The EG method defined in (7) satisfies discrete local mass and energy equations.*

Proof To derive a discrete counterpart of (12a), take $w = \mathbf{1}_K$ in (7b), where $\mathbf{1}_K$ is a characteristic function. Then, using the fact that $\nabla w = 0$ and the divergence theorem, we can obtain

$$\begin{aligned} & - \langle \left\{ \mathbf{K} \nabla p_h^{n+1} \cdot \mathbf{n}_K \right\}, 1 \rangle_{\partial K} + \beta^p \langle h_e^{-1} \left[\left[p_h^{n+1} \right] \right], 1 \rangle_{\partial K} \\ &= (g^{n+1}, 1)_K - c_0(D_t p_h^{n+1}, 1)_K - \alpha \langle \left\{ D_t \mathbf{u}_h^{n+1} \cdot \mathbf{n}_K \right\}, 1 \rangle_{\partial K} + 3\alpha_m (D_t \theta_h^{n+1}, 1)_K. \end{aligned}$$

Therefore, by defining the normal component of our numerical fluid flux $\mathbf{q}_{p,h}^{n+1}$ by

$$\mathbf{q}_{p,h}^{n+1} \cdot \mathbf{n}_K = - \left\{ \mathbf{K} \nabla p_h^{n+1} \cdot \mathbf{n}_K \right\} + \beta^p h_e^{-1} \left[\left[p_h^{n+1} \right] \right],$$

we can obtain a discrete counterpart of (12a):

$$\begin{aligned} \langle \mathbf{q}_{p,h}^{n+1} \cdot \mathbf{n}_K, 1 \rangle_{\partial K} &= (g^{n+1}, 1)_K - c_0(D_t p_h^{n+1}, 1)_K - \alpha \langle \left\{ D_t \mathbf{u}_h^{n+1} \cdot \mathbf{n}_K \right\}, 1 \rangle_{\partial K} \\ &\quad + 3\alpha_m (D_t \theta_h^{n+1}, 1)_K. \end{aligned} \quad (13a)$$

Similarly, by defining our numerical thermal flux $\mathbf{q}_{\theta,h}^{n+1}$ by

$$\mathbf{q}_{\theta,h}^{n+1} \cdot \mathbf{n}_K = - \left\{ \mathbf{D} \nabla \theta_h^{n+1} \cdot \mathbf{n}_K \right\} + \beta^\theta h_e^{-1} \left[\left[\theta_h^{n+1} \right] \right],$$

we can obtain a discrete counterpart of (12b):

$$\begin{aligned} \langle \mathbf{q}_{\theta,h}^{n+1} \cdot \mathbf{n}_K, 1 \rangle_{\partial K} &= (\eta^{n+1}, 1)_K - C_d(D_t \theta_h^{n+1}, 1)_K \\ &\quad - 3\alpha_T K_{dr} \theta_0 \langle \left\{ D_t \mathbf{u}_h^{n+1} \cdot \mathbf{n}_K \right\}, 1 \rangle_{\partial K} + 3\alpha_m \theta_0 (D_t p_h^{n+1}, 1)_K. \end{aligned} \quad (13b)$$

□

5 A Priori Error Estimates

In this section, we establish the error estimates for the fully discrete EG method. To define an approximate initial solution $(\mathbf{u}_h^0, p_h^0, \theta_h^0)$ and to aid our convergence analysis, we first consider the following elliptic projection $(\bar{\mathbf{u}}_h, \bar{p}_h, \bar{\theta}_h) \in \mathbf{V}_h \times \mathcal{W}_h \times \mathcal{W}_h$ of the true solution (\mathbf{u}, p, θ) defined by:

$$\mathbf{a}_h^{\mathbf{u}}(\bar{\mathbf{u}}_h, \mathbf{v}) = \mathbf{a}_h^{\mathbf{u}}(\mathbf{u}, \mathbf{v}) \quad \mathbf{v} \in \mathbf{V}_h, \quad (14a)$$

$$\mathbf{a}_h^p(\bar{p}_h, w) = \mathbf{a}_h^p(p, w) \quad w \in \mathcal{W}_h, \quad (14b)$$

$$\mathbf{a}_h^\theta(\bar{\theta}_h, s) = \mathbf{a}_h^\theta(\theta, s) \quad s \in \mathcal{W}_h. \quad (14c)$$

Assume that our numerical solution at the initial time $t = 0$ is defined by elliptic projections of the initial solutions given in (5):

$$\mathbf{u}_h^0 = \bar{\mathbf{u}}_h^0, \quad p_h^0 = \bar{p}_h^0, \quad \text{and} \quad \theta_h^0 = \bar{\theta}_h^0. \quad (15)$$

Then, we have the following error estimates.

Theorem 5.1 *For $1 \leq n \leq N$, let $(\mathbf{u}^n, p^n, \theta^n)$ be the true solution and $(\mathbf{u}_h^n, p_h^n, \theta_h^n)$ be the numerical solution of the EG method at time t^n . Assume that the true solution and initial and boundary data satisfy sufficient regularity conditions and that $c_0 - 3\alpha_m > 0$ and $C_d - 3\alpha_m\theta_0 > 0$. Then, provided that the penalty parameters $\beta^{\mathbf{u}}, \beta^p$, and β^θ are large enough and $\Delta t = \mathcal{O}(h) \ll 1$, we have the following optimal a priori error estimates:*

$$\begin{aligned} & \max_{1 \leq n \leq N} \|\mathbf{u}^n - \mathbf{u}_h^n\|_{\mathcal{V}}^2 + \Delta t \sum_{n=1}^N \left(\|p^n - p_h^n\|_{\mathcal{W}}^2 + \|\theta^n - \theta_h^n\|_{\mathcal{W}}^2 \right) \\ & \leq C \left[h^2 \left(\|\mathbf{u}^0\|_2^2 + \|p^0\|_2^2 + \|\theta^0\|_2^2 + \|\mathbf{u}_t\|_{L^2(0,T; H^2(\Omega))}^2 + \|p_t\|_{L^2(0,T; H^1(\Omega))}^2 \right. \right. \\ & \quad \left. \left. + \|\theta_t\|_{L^2(0,T; H^1(\Omega))}^2 \right) + (\Delta t)^2 \left(\|\mathbf{u}_{tt}\|_{L^2(0,T; H^1(\Omega))}^2 + \|\mathbf{u}_{tt}\|_{L^2(0,T; L^2(\partial\Omega))}^2 \right. \right. \\ & \quad \left. \left. + \|p_{tt}\|_{L^2(0,T; L^2(\Omega))}^2 + \|\theta_{tt}\|_{L^2(0,T; L^2(\Omega))}^2 \right) \right]. \end{aligned} \quad (16)$$

The proof of this theorem will be conducted in several steps. First, note that the errors in the solution variables can be split into two parts:

$$\mathbf{u} - \mathbf{u}_h = \chi_{\mathbf{u}} + \xi_{\mathbf{u}}, \quad p - p_h = \chi_p + \xi_p, \quad \theta - \theta_h = \chi_\theta + \xi_\theta,$$

where

$$\begin{aligned} \chi_{\mathbf{u}} &= \mathbf{u} - \bar{\mathbf{u}}_h, & \chi_p &= p - \bar{p}_h, & \chi_\theta &= \theta - \bar{\theta}_h, \\ \xi_{\mathbf{u}} &= \bar{\mathbf{u}}_h - \mathbf{u}_h, & \xi_p &= \bar{p}_h - p_h, & \xi_\theta &= \bar{\theta}_h - \theta_h. \end{aligned}$$

We will first analyze the auxiliary error at the first time step, $(\xi_{\mathbf{u}}^1, \xi_p^1, \xi_\theta^1)$, then use it to analyze the errors at subsequent steps. Then, the main result, (16), is a consequence of the error estimates of the elliptic projections to be proved in subsection 5, the auxiliary error estimates (32) to be proved in subsection 5, and the triangle inequality.

5.1 Preliminary lemmas

In this subsection, we will present some useful lemmas to be repeatedly used in our analysis. First, one key ingredient for the error estimates is the interpolation operators $\Pi_h^{\mathcal{V}} : [H^1(\Omega)]^d \rightarrow \mathcal{V}_h$ and $\Pi_h^{\mathcal{W}} : H^1(\Omega) \rightarrow \mathcal{W}_h$. They are defined

in [18, Section 4] and [14] and their useful properties and error estimates are studied there too. To make our paper self-contained, we present them here without proof.

Lemma 5.1 *There exists an interpolation operator $\Pi_h^{\mathcal{V}} : [H^1(\Omega)]^d \rightarrow \mathcal{V}_h$ that satisfies*

$$(\nabla \cdot (\mathbf{v} - \Pi_h^{\mathcal{V}} \mathbf{v}), 1)_K = 0 \quad \forall K \in \mathcal{T}_h, \quad (17a)$$

$$|\mathbf{v} - \Pi_h^{\mathcal{V}} \mathbf{v}|_j \leq Ch^{m-j} |\mathbf{v}|_m, \quad 0 \leq j \leq m \leq 2, \quad \forall \mathbf{v} \in [H^2(\Omega)]^d, \quad (17b)$$

$$|\nabla \cdot (\mathbf{v} - \Pi_h^{\mathcal{V}} \mathbf{v})|_j \leq Ch^{1-j} |\nabla \cdot \mathbf{v}|_1, \quad 0 \leq j \leq 1, \quad \forall \mathbf{v} \in [H^2(\Omega)]^d, \quad (17c)$$

$$\|\Pi_h^{\mathcal{V}} \mathbf{v}\|_{\mathcal{V}} \leq C \|\mathbf{v}\|_1 \quad \forall \mathbf{v} \in [H_{0,\Gamma_d}^1(\Omega)]^d, \quad (17d)$$

$$\|\mathbf{v} - \Pi_h^{\mathcal{V}} \mathbf{v}\|_{\mathcal{V}} \leq Ch^{m-1} \|\mathbf{v}\|_m, \quad 1 \leq m \leq 2 \quad \forall \mathbf{v} \in [H^2(\Omega)]^d, \quad (17e)$$

where $C > 0$ is a generic constant independent of h .

Lemma 5.2 *There exists an interpolation operator $\Pi_h^{\mathcal{W}} : H^1(\Omega) \rightarrow \mathcal{W}_h$ that satisfies*

$$(w - \Pi_h^{\mathcal{W}} w, 1)_K = 0 \quad \forall K \in \mathcal{T}_h, \quad (18a)$$

$$|w - \Pi_h^{\mathcal{W}} w|_j \leq Ch^{m-j} |w|_m, \quad 0 \leq j \leq m \leq 2 \quad \forall w \in H^2(\Omega), \quad (18b)$$

$$\|w - \Pi_h^{\mathcal{W}} w\|_{\mathcal{W}} \leq Ch \|w\|_2 \quad \forall w \in H^2(\Omega). \quad (18c)$$

Lemma 5.3 *We have the following error estimates for the elliptic projection $(\bar{\mathbf{u}}_h, \bar{p}_h, \bar{\theta}_h)$ defined in (14):*

$$\|\mathbf{u} - \bar{\mathbf{u}}_h\|_0 + h \|\mathbf{u} - \bar{\mathbf{u}}_h\|_{\mathcal{V}} \leq Ch^2 \|\mathbf{u}\|_2, \quad (19a)$$

$$\|p - \bar{p}_h\|_0 + h \|p - \bar{p}_h\|_{\mathcal{W}} \leq Ch^2 \|p\|_2, \quad (19b)$$

$$\|\theta - \bar{\theta}_h\|_0 + h \|\theta - \bar{\theta}_h\|_{\mathcal{W}} \leq Ch^2 \|\theta\|_2. \quad (19c)$$

Proof To prove the energy norm error estimate in (19a), first subtract $\mathbf{a}_h^{\mathbf{u}}(\Pi_h^{\mathcal{V}} \mathbf{u}, \mathbf{v})$ from both sides of (14a) to get

$$\mathbf{a}_h^{\mathbf{u}}(\bar{\mathbf{u}}_h - \Pi_h^{\mathcal{V}} \mathbf{u}, \mathbf{v}) = \mathbf{a}_h^{\mathbf{u}}(\mathbf{u} - \Pi_h^{\mathcal{V}} \mathbf{u}, \mathbf{v}).$$

Take $\mathbf{v} = \bar{\mathbf{u}}_h - \Pi_h^{\mathcal{V}} \mathbf{u}$ and use the coercivity condition (10a) and the continuity condition (8a) on the left- and right-hand side of the above equation, respectively, to obtain

$$\kappa_{\mathbf{u}} \|\bar{\mathbf{u}}_h - \Pi_h^{\mathcal{V}} \mathbf{u}\|_{\mathcal{V}}^2 \leq C_{a_{\mathbf{u}}} \|\mathbf{u} - \Pi_h^{\mathcal{V}} \mathbf{u}\|_{\mathcal{V}} \|\bar{\mathbf{u}}_h - \Pi_h^{\mathcal{V}} \mathbf{u}\|_{\mathcal{V}}.$$

This inequality, together with (17e), yields

$$\|\bar{\mathbf{u}}_h - \Pi_h^{\mathcal{V}} \mathbf{u}\|_{\mathcal{V}} \leq Ch \|\mathbf{u}\|_2.$$

Then, the desired error bound can be obtained by using the triangle inequality. We can prove the energy norm error estimates for \bar{p}_h and $\bar{\theta}_h$ in (19b) and (19c) in the same manner. Using these results in the standard duality arguments, we can prove the L^2 -norm error estimates. \square

Lemma 5.4 Let $\phi \in C^2(0, T; H^m(\mathcal{T}_h))$ be a scalar or vector-valued function for some $m > 0$, and let E be a set belonging to either \mathcal{E}_h or \mathcal{T}_h . Then, we have the following Taylor expansions and error bounds:

$$\phi^n = \phi^0 + \int_0^{t^n} \phi_t(s) ds, \quad (20a)$$

$$D_t \phi^{n+1} = \frac{1}{\Delta t} \int_{t^n}^{t^{n+1}} \phi_t(s) ds, \quad (20b)$$

$$D_t \phi^{n+1} = \phi_t^{n+1} + \frac{1}{\Delta t} \int_{t^n}^{t^{n+1}} (s - t^n) \phi_{tt}(s) ds, \quad (20c)$$

and

$$\|\phi^n\|_{j,E} \leq C(\|\phi^0\|_{j,E} + \|\phi_t\|_{L^2(0,t^n; H^j(E))}), \quad 0 \leq j \leq m, \quad (21a)$$

$$\|D_t \phi^{n+1}\|_{j,E} \leq (\Delta t)^{-\frac{1}{2}} \|\phi_t\|_{L^2(t^n, t^{n+1}; H^j(E))}, \quad 0 \leq j \leq m, \quad (21b)$$

$$\|D_t \phi^{n+1} - \phi_t^{n+1}\|_{j,E} \leq (\Delta t)^{\frac{1}{2}} \|\phi_{tt}\|_{L^2(t^n, t^{n+1}; H^j(E))}, \quad 0 \leq j \leq m. \quad (21c)$$

Note that the error estimates in (21b) are particularly true for $\phi = \chi_\psi$, where $\psi = \mathbf{u}, p$, or θ . Hence, we have the following corollary.

Corollary 5.1 Let $\psi = \mathbf{u}, p$, or θ . Then, on any set E belonging to either \mathcal{E}_h or \mathcal{T}_h ,

$$\|D_t \chi_\psi^{n+1}\|_{j,E} \leq (\Delta t)^{-\frac{1}{2}} \|\chi_{\psi_t}\|_{L^2(t^n, t^{n+1}; H^j(E))}, \quad j = 0, 1. \quad (22)$$

Another inequality to be used frequently in our analysis is the following:

Lemma 5.5 For any symmetric bilinear form \mathbf{c} on $X \times X$ for some Hilbert space X , we have

$$\mathbf{c}(a - b, a) \geq \frac{1}{2}(\mathbf{c}(a, a) - \mathbf{c}(b, b)) \quad \forall a, b \in X. \quad (23)$$

5.2 Auxiliary error estimates

Lemma 5.6 For $0 \leq n \leq N - 1$, let $(\mathbf{u}^{n+1}, p^{n+1}, \theta^{n+1})$ be the true solution and $(\mathbf{u}_h^{n+1}, p_h^{n+1}, \theta_h^{n+1})$ be the numerical solution of the EG method. Then, they satisfy the following equations:

$$\begin{aligned} \mathbf{a}_h(\xi_{\mathbf{u}}^{n+1}, \mathbf{v}) - \alpha \mathbf{b}_h(\mathbf{v}, \xi_p^{n+1}) - 3\alpha_T K_{dr} \mathbf{b}_h(\mathbf{v}, \xi_\theta^{n+1}) \\ = \alpha \mathbf{b}_h(\mathbf{v}, \chi_p^{n+1}) + 3\alpha_T K_{dr} \mathbf{b}_h(\mathbf{v}, \chi_\theta^{n+1}), \end{aligned} \quad (24a)$$

$$\begin{aligned} c_0(D_t \xi_p^{n+1}, w)_{\mathcal{T}_h} + \alpha \mathbf{b}_h(D_t \xi_{\mathbf{u}}^{n+1}, w) - 3\alpha_m(D_t \xi_\theta^{n+1}, w)_{\mathcal{T}_h} + \mathbf{a}_h^p(\xi_p^{n+1}, w) \\ = -c_0(D_t \chi_p^{n+1}, w)_{\mathcal{T}_h} - \alpha \mathbf{b}_h(D_t \chi_{\mathbf{u}}^{n+1}, w) + 3\alpha_m(D_t \chi_\theta^{n+1}, w)_{\mathcal{T}_h} \\ + c_0(D_t p^{n+1} - p_t^{n+1}, w)_{\mathcal{T}_h} + \alpha \mathbf{b}_h(D_t \mathbf{u}^{n+1} - \mathbf{u}_t^{n+1}, w) \\ - 3\alpha_m(D_t \theta^{n+1} - \theta_t^{n+1}, w)_{\mathcal{T}_h}, \end{aligned} \quad (24b)$$

$$C_d(D_t \xi_\theta^{n+1}, s)_{\mathcal{T}_h} + 3\alpha_T K_{dr} \theta_0 \mathbf{b}_h(D_t \xi_{\mathbf{u}}^{n+1}, s) - 3\alpha_m \theta_0(D_t \xi_p^{n+1}, s)_{\mathcal{T}_h} + \mathbf{a}_h^\theta(\xi_\theta^{n+1}, s)$$

$$\begin{aligned}
&= -C_d(D_t \chi_\theta^{n+1}, s)_{\mathcal{T}_h} - 3\alpha_T K_{dr} \theta_0 \mathbf{b}_h(D_t \chi_\mathbf{u}^{n+1}, s) + 3\alpha_m \theta_0(D_t \chi_p^{n+1}, s)_{\mathcal{T}_h} \\
&\quad + C_d(D_t \theta^{n+1} - \theta_t^{n+1}, s)_{\mathcal{T}_h} + 3\alpha_T K_{dr} \theta_0 \mathbf{b}_h(D_t \mathbf{u}^{n+1} - \mathbf{u}_t^{n+1}, s) \\
&\quad - 3\alpha_m \theta_0(D_t p^{n+1} - p_t^{n+1}, s)_{\mathcal{T}_h}, \tag{24c}
\end{aligned}$$

Proof It is easy to check that the true solution (\mathbf{u}, p, θ) satisfies the following system at time t^{n+1} :

$$\mathbf{a}_h^\mathbf{u}(\mathbf{u}^{n+1}, \mathbf{v}) - \alpha \mathbf{b}_h(\mathbf{v}, p^{n+1}) - 3\alpha_T K_{dr} \mathbf{b}_h(\mathbf{v}, \theta^{n+1}) = \mathbf{g}_h^\mathbf{u}(t^{n+1} \mathbf{v}), \tag{25a}$$

$$c_0(p_t^{n+1}, w)_{\mathcal{T}_h} + \alpha \mathbf{b}_h(\mathbf{u}_t^{n+1}, w) - 3\alpha_m(\theta_t^{n+1}, w)_{\mathcal{T}_h} + \mathbf{a}_h^p(p^{n+1}, w) = \mathbf{g}_h^p(t^{n+1}; w), \tag{25b}$$

$$\begin{aligned}
C_d(\theta_t^{n+1}, s)_{\mathcal{T}_h} + 3\alpha_T K_{dr} \theta_0 \mathbf{b}_h(\mathbf{u}_t^{n+1}, s) - 3\alpha_m \theta_0(p_t^{n+1}, s)_{\mathcal{T}_h} + \mathbf{a}_h^\theta(\theta^{n+1}, s) \\
= \mathbf{g}_h^\theta(t^{n+1}; s) \tag{25c}
\end{aligned}$$

for $\forall (\mathbf{v}, w, s) \in \mathbf{V}_h \times \mathcal{W}_h \times \mathcal{W}_h$. Subtracting (7) from (25) and doing some algebraic manipulations, we obtain the desired error equations in (24). \square

We will first analyze the auxiliary error at the first time step, $(\xi_\mathbf{u}^1, \xi_p^1, \xi_\theta^1)$, then use it to analyze the errors at subsequent steps.

Lemma 5.7 *Assume that*

$$c_0 > 3\alpha_m \quad \text{and} \quad C_d > 3\alpha_m \theta_0. \tag{26}$$

Then, provided that the penalty parameters $\beta^\mathbf{u}$, β^p , and β^θ are large enough, we have the following auxiliary error estimates:

$$\begin{aligned}
&\|\xi_\mathbf{u}^1\|_{\mathcal{V}}^2 + \|\xi_p^1\|_{\mathcal{W}}^2 + \|\xi_\theta^1\|_{\mathcal{W}}^2 + \|\xi_p^1\|_0^2 + \|\xi_\theta^1\|_0^2 \\
&\leq C \left[h^2 \left(\|p^0\|_1^2 + \|\theta^0\|_1^2 + \|\mathbf{u}_t\|_{L^2(0, \Delta t; H^1(\Omega))}^2 + \|p_t\|_{L^2(0, \Delta t; H^1(\Omega))}^2 \right. \right. \\
&\quad \left. \left. + \|\theta_t\|_{L^2(0, \Delta t; H^1(\Omega))}^2 \right) + (\Delta t)^2 \left(\|\mathbf{u}_{tt}\|_{L^2(0, \Delta t; L^2(\Omega))}^2 + \|p_{tt}\|_{L^2(0, \Delta t; L^2(\Omega))}^2 \right. \right. \\
&\quad \left. \left. + \|\theta_{tt}\|_{L^2(0, \Delta t; L^2(\Omega))}^2 \right) \right]. \tag{27}
\end{aligned}$$

Proof Consider (24) with $n = 0$. Take $(\mathbf{v}, w, s) = (\theta_0 \xi_\mathbf{u}^1, \theta_0 \Delta t \xi_p^1, \Delta t \xi_\theta^1)$ in the equation and use $(\xi_\mathbf{u}^0, \xi_p^0, \xi_\theta^0) = (\mathbf{0}, 0, 0)$, then add the three resulting equations to obtain

$$\begin{aligned}
&\theta_0 \mathbf{a}_h^\mathbf{u}(\xi_\mathbf{u}^1, \xi_\mathbf{u}^1) + \theta_0 \Delta t \mathbf{a}_h^p(\xi_p^1, \xi_p^1) + \Delta t \mathbf{a}_h^\theta(\xi_\theta^1, \xi_\theta^1) + c_0 \theta_0(\xi_p^1, \xi_p^1)_{\mathcal{T}_h} \\
&\quad + C_d(\xi_\theta^1, \xi_\theta^1)_{\mathcal{T}_h} - 6\alpha_m \theta_0(\xi_\theta^1, \xi_p^1)_{\mathcal{T}_h} \\
&= \theta_0 \alpha \mathbf{b}_h(\xi_\mathbf{u}^1, \chi_\mathbf{u}^1) + 3\theta_0 \alpha_T K_{dr} \mathbf{b}_h(\xi_\mathbf{u}^1, \chi_\theta^1) - \alpha \theta_0 \Delta t \mathbf{b}_h(D_t \chi_\mathbf{u}^1, \xi_p^1) \\
&\quad - 3\alpha_T K_{dr} \theta_0 \Delta t \mathbf{b}_h(D_t \chi_\mathbf{u}^1, \xi_\theta^1) + \alpha \theta_0 \Delta t \mathbf{b}_h(D_t \mathbf{u}^1 - \mathbf{u}_t^1, \xi_p^1) \\
&\quad + 3\alpha_T K_{dr} \theta_0 \Delta t \mathbf{b}_h(D_t \mathbf{u}^1 - \mathbf{u}_t^1, \xi_\theta^1) - c_0 \theta_0 \Delta t (D_t \chi_\mathbf{u}^1, \xi_p^1)_{\mathcal{T}_h} + 3\alpha_m \Delta t \theta_0 (D_t \chi_p^1, \xi_\theta^1)_{\mathcal{T}_h} \\
&\quad - C_d \Delta t (D_t \chi_\theta^1, \xi_\theta^1)_{\mathcal{T}_h} + 3\alpha_m \theta_0 \Delta t (D_t \chi_\theta^1, \xi_p^1)_{\mathcal{T}_h} + c_0 \theta_0 \Delta t (D_t p^1 - p_t^1, \xi_p^1)_{\mathcal{T}_h} \\
&\quad - 3\alpha_m \theta_0 \Delta t (D_t p^1 - p_t^1, \xi_\theta^1)_{\mathcal{T}_h} + C_d \Delta t (D_t \theta^1 - \theta_t^1, \xi_\theta^1)_{\mathcal{T}_h}
\end{aligned}$$

$$-3\alpha_m\theta_0\Delta t(D_t\theta^1 - \theta_t^1, \xi_p^1)_{\mathcal{T}_h} := \sum_{i=1}^{14} \phi_i. \quad (28)$$

We can bound below the left-hand side (LHS) of (28) using the coercivity conditions in (10) for the first three terms and applying the Cauchy-Schwarz and Young's inequalities to the last term to obtain the following lower bound:

$$\begin{aligned} LHS &\geq \theta_0\kappa_{\mathbf{u}}\|\xi_{\mathbf{u}}^1\|_{\mathcal{V}}^2 + \theta_0\kappa_p\Delta t\|\xi_p^1\|_{\mathcal{W}}^2 + \kappa_{\theta}\Delta t\|\xi_{\theta}^1\|_{\mathcal{W}}^2 \\ &\quad + (c_0 - 3\alpha_m)\theta_0\|\xi_p^1\|_0^2 + (C_d - 3\alpha_m\theta_0)\|\xi_{\theta}^1\|_0^2. \end{aligned}$$

We also want to bound the right-hand side of (28). Applying (9a) to the first two terms and (9b) to the next four terms, then using the Cauchy-Schwarz and Young's inequalities, (19), and (21), we can bound the first six terms as follows:

$$\begin{aligned} \sum_{i=1}^6 \phi_i &\leq \frac{1}{2}(\theta_0\kappa_{\mathbf{u}}\|\xi_{\mathbf{u}}^1\|_{\mathcal{V}}^2 + \theta_0\kappa_p\Delta t\|\xi_p^1\|_{\mathcal{W}}^2 + \kappa_{\theta}\Delta t\|\xi_{\theta}^1\|_{\mathcal{W}}^2) \\ &\quad + C(\|\chi_p^1\|_0^2 + \|\chi_{\theta}^1\|_0^2 + \Delta t\|D_t\chi_{\mathbf{u}}^1\|_0^2 + \Delta t\|D_t\mathbf{u}^1 - \mathbf{u}_t^1\|_0^2) \\ &\leq \frac{1}{2}(\theta_0\kappa_{\mathbf{u}}\|\xi_{\mathbf{u}}^1\|_{\mathcal{V}}^2 + \theta_0\kappa_p\Delta t\|\xi_p^1\|_{\mathcal{W}}^2 + \kappa_{\theta}\Delta t\|\xi_{\theta}^1\|_{\mathcal{W}}^2) \\ &\quad + C\left[h^2\left(\|p^1\|_1^2 + \|\theta^1\|_1^2 + \|\mathbf{u}_t\|_{L^2(0,\Delta t; H^1(\Omega))}^2\right) + (\Delta t)^2\|\mathbf{u}_{tt}\|_{L^2(0,\Delta t; L^2(\Omega))}^2\right] \\ &\leq \frac{1}{2}(\theta_0\kappa_{\mathbf{u}}\|\xi_{\mathbf{u}}^1\|_{\mathcal{V}}^2 + \theta_0\kappa_p\Delta t\|\xi_p^1\|_{\mathcal{W}}^2 + \kappa_{\theta}\Delta t\|\xi_{\theta}^1\|_{\mathcal{W}}^2) \\ &\quad + C\left[h^2\left(\|p^0\|_1^2 + \|\theta^0\|_1^2 + \|\mathbf{u}_t\|_{L^2(0,\Delta t; H^1(\Omega))}^2\right) + (\Delta t)^2\|\mathbf{u}_{tt}\|_{L^2(0,\Delta t; L^2(\Omega))}^2\right]. \end{aligned}$$

The rest of the terms can be bounded similarly.

$$\begin{aligned} \sum_{i=7}^{14} \phi_i &\leq \epsilon_1\Delta t\theta_0\|\xi_p^1\|_0^2 + \epsilon_2\Delta t\|\xi_{\theta}^1\|_0^2 \\ &\quad + C\Delta t(\|D_t\chi_p^1\|_0^2 + \|D_t\chi_{\theta}^1\|_0^2 + \|D_t p^1 - p_t^1\|_0^2 + \|D_t\theta^1 - \theta_t^1\|_0^2) \\ &\leq \epsilon_1\Delta t\theta_0\|\xi_p^1\|_0^2 + \epsilon_2\Delta t\|\xi_{\theta}^1\|_0^2 + C\left[h^2\left(\|p_t\|_{L^2(0,\Delta t; H^1(\Omega))}^2 + \|\theta_t\|_{L^2(0,\Delta t; H^1(\Omega))}^2\right) \right. \\ &\quad \left. + (\Delta t)^2\left(\|p_{tt}\|_{L^2(0,\Delta t; L^2(\Omega))}^2 + \|\theta_{tt}\|_{L^2(0,\Delta t; L^2(\Omega))}^2\right)\right]. \end{aligned}$$

Putting together the lower-bound and upper-bound of (28), we have

$$\begin{aligned} &\theta_0\kappa_{\mathbf{u}}\|\xi_{\mathbf{u}}^1\|_{\mathcal{V}}^2 + \theta_0\kappa_p\Delta t\|\xi_p^1\|_{\mathcal{W}}^2 + \kappa_{\theta}\Delta t\|\xi_{\theta}^1\|_{\mathcal{W}}^2 \\ &\quad + (c_0 - 3\alpha_m - \epsilon_1\Delta t)\theta_0\|\xi_p^1\|_0^2 + (C_d - 3\alpha_m\theta_0 - \epsilon_2\Delta t)\|\xi_{\theta}^1\|_0^2 \\ &\leq C\left[h^2\left(\|p^0\|_1^2 + \|\theta^0\|_1^2 + \|\mathbf{u}_t\|_{L^2(0,\Delta t; H^1(\Omega))}^2 + \|p_t\|_{L^2(0,\Delta t; H^1(\Omega))}^2 \right. \right. \\ &\quad \left. \left. + \|\theta_t\|_{L^2(0,\Delta t; H^1(\Omega))}^2\right) + (\Delta t)^2\left(\|\mathbf{u}_{tt}\|_{L^2(0,\Delta t; L^2(\Omega))}^2 + \|p_{tt}\|_{L^2(0,\Delta t; L^2(\Omega))}^2 \right. \right. \\ &\quad \left. \left. + \|\theta_{tt}\|_{L^2(0,\Delta t; L^2(\Omega))}^2\right)\right] \end{aligned}$$

for some positive constants ϵ_1 and ϵ_2 . Thanks to the assumptions in (26), the coefficients in front of $\|\xi_p^1\|_0^2$ and $\|\xi_{\theta}^1\|_0^2$ can be made positive for sufficiently small ϵ_1 and ϵ_2 . Therefore, we obtain the desired error estimate. \square

Lemma 5.8 *Assume the conditions in (26), i.e., $c_0 - 3\alpha_m > 0$ and $C_d - 3\alpha_m\theta_0 > 0$, and that the penalty parameters β^u , β^p , and β^θ are large enough. Then, we have the following auxiliary error estimates:*

$$\begin{aligned} & \max_{2 \leq n \leq N} \|\xi_p^n\|_{\mathcal{W}}^2 + \max_{2 \leq n \leq N} \|\xi_\theta^n\|_{\mathcal{W}}^2 + \Delta t \sum_{n=2}^N \left(\|D_t \xi_u^{n+1}\|_{\mathcal{V}}^2 + \|D_t \xi_p^n\|_0^2 + \|D_t \xi_\theta^n\|_0^2 \right) \\ & \leq C \left[h^2 \left(\|p^0\|_1^2 + \|\theta^0\|_1^2 + \|\mathbf{u}_t\|_{L^2(0,T; H^2(\Omega))}^2 + \|p_t\|_{L^2(0,T; H^1(\Omega))}^2 \right. \right. \\ & \quad \left. \left. + \|\theta_t\|_{L^2(0,T; H^1(\Omega))}^2 \right) + (\Delta t)^2 \left(\|\mathbf{u}_{tt}\|_{L^2(0,T; H^1(\Omega))}^2 + \frac{1}{h} \|\mathbf{u}_{tt}\|_{L^2(0,T; L^2(\partial\Omega))}^2 \right. \right. \\ & \quad \left. \left. + \|p_{tt}\|_{L^2(0,T; L^2(\Omega))}^2 + \|\theta_{tt}\|_{L^2(0,T; L^2(\Omega))}^2 \right) \right]. \end{aligned} \quad (29)$$

Proof First note that (24a) holds at every time step n , $1 \leq n \leq N-1$. Therefore, we can obtain the following equation with the discrete time derivative for $1 \leq n \leq N-1$:

$$\begin{aligned} & \mathbf{a}_h^u(D_t \xi_u^{n+1}, \mathbf{v}) - \alpha \mathbf{b}_h(\mathbf{v}, D_t \xi_p^{n+1}) - 3\alpha_T K_{dr} \mathbf{b}_h(\mathbf{v}, D_t \xi_\theta^{n+1}) \\ & = -\mathbf{a}_h^u(D_t \chi_u^{n+1}, \mathbf{v}) + \alpha \mathbf{b}_h(\mathbf{v}, D_t \chi_p^{n+1}) + 3\alpha_T K_{dr} \mathbf{b}_h(\mathbf{v}, D_t \chi_\theta^{n+1}). \end{aligned} \quad (30)$$

Take $\mathbf{v} = \theta_0 \Delta t D_t \xi_u^{n+1}$, $w = \theta_0 \Delta t D_t \xi_p^{n+1}$, and $s = \Delta t D_t \xi_\theta^{n+1}$ in (30), (24b), and (24c), respectively, add the three equations, then use the definitions of the elliptic projections in (14), rearrange the terms to collect the terms in a similar form so that we can analyze multiple terms together. Then, we can obtain

$$\begin{aligned} & \theta_0 \Delta t \mathbf{a}_h^u(D_t \xi_u^{n+1}, D_t \xi_u^{n+1}) + \theta_0 \mathbf{a}_h^p(\xi_p^{n+1}, \xi_p^{n+1} - \xi_p^n) + \mathbf{a}_h^\theta(\xi_\theta^{n+1}, \xi_\theta^{n+1} - \xi_\theta^n) \\ & + c_0 \theta_0 \Delta t (D_t \xi_p^{n+1}, D_t \xi_p^{n+1})_{\mathcal{T}_h} + C_d \Delta t (D_t \xi_\theta^{n+1}, D_t \xi_\theta^{n+1})_{\mathcal{T}_h} \\ & - 6\alpha_m \theta_0 \Delta t (D_t \xi_\theta^{n+1}, D_t \xi_p^{n+1})_{\mathcal{T}_h} \\ & = \alpha \theta_0 \Delta t \mathbf{b}_h(D_t \xi_u^{n+1}, D_t \chi_p^{n+1}) + 3\alpha_T K_{dr} \theta_0 \Delta t \mathbf{b}_h(D_t \xi_u^{n+1}, D_t \chi_\theta^{n+1}) \\ & - \alpha \theta_0 \Delta t \mathbf{b}_h(D_t \chi_u^{n+1}, D_t \xi_p^{n+1}) - 3\alpha_T K_{dr} \theta_0 \Delta t \mathbf{b}_h(D_t \chi_u^{n+1}, D_t \xi_\theta^{n+1}) \\ & + \alpha \theta_0 \Delta t \mathbf{b}_h(D_t \mathbf{u}^{n+1} - \mathbf{u}_t^{n+1}, D_t \xi_p^{n+1}) + 3\alpha_T K_{dr} \theta_0 \Delta t \mathbf{b}_h(D_t \mathbf{u}^{n+1} - \mathbf{u}_t^{n+1}, D_t \xi_\theta^{n+1}) \\ & - c_0 \theta_0 \Delta t (D_t \chi_p^{n+1}, D_t \xi_p^{n+1})_{\mathcal{T}_h} + 3\alpha_m \theta_0 \Delta t (D_t \chi_p^{n+1}, D_t \xi_\theta^{n+1})_{\mathcal{T}_h} \\ & + 3\alpha_m \theta_0 \Delta t (D_t \chi_\theta^{n+1}, D_t \xi_p^{n+1})_{\mathcal{T}_h} - C_d \theta_0 \Delta t (D_t \chi_\theta^{n+1}, D_t \xi_\theta^{n+1})_{\mathcal{T}_h} \\ & + c_0 \theta_0 \Delta t (D_t p^{n+1} - p_t^{n+1}, D_t \xi_p^{n+1})_{\mathcal{T}_h} - 3\alpha_m \theta_0 \Delta t \theta_0 (D_t p^{n+1} - p_t^{n+1}, D_t \xi_\theta^{n+1})_{\mathcal{T}_h} \\ & - 3\alpha_m \theta_0 \Delta t (D_t \theta^{n+1} - \theta_t^{n+1}, D_t \xi_p^{n+1})_{\mathcal{T}_h} + C_d \Delta t (D_t \theta^{n+1} - \theta_t^{n+1}, D_t \xi_\theta^{n+1})_{\mathcal{T}_h} \\ & := \sum_{i=1}^{14} \Phi_i. \end{aligned}$$

Now, take summation over time from $n = 1$ to $M-1$ on both sides for an arbitrary integer $2 \leq M \leq N$. Then, using the Cauchy-Schwarz and Young's inequalities, (23), and the coercivity and continuity of the bilinear forms, the left-hand side is bounded below by

$$LHS \geq \theta_0 \kappa_u \Delta t \sum_{n=1}^{M-1} \|D_t \xi_u^{n+1}\|_{\mathcal{V}}^2 + \frac{\theta_0}{2} (\kappa_p \|\xi_p^M\|_{\mathcal{W}}^2 - C_{a_p} \|\xi_p^1\|_{\mathcal{W}}^2)$$

$$\begin{aligned}
& + \frac{1}{2}(\kappa_\theta \|\xi_\theta^M\|_{\mathcal{W}}^2 - C_{a_\theta} \|\xi_\theta^1\|_{\mathcal{W}}^2) + (c_0 - 3\alpha_m)\theta_0 \Delta t \sum_{n=1}^{M-1} \|D_t \xi_p^{n+1}\|_0^2 \\
& + (C_d - 3\alpha_m \theta_0) \Delta t \sum_{n=1}^{M-1} \|D_t \xi_\theta^{n+1}\|_0^2. \tag{31}
\end{aligned}$$

We also need to bound the right-hand side. For the first four terms, we use the continuity condition (9a) of the bilinear form \mathbf{b}_h , then apply the Cauchy-Schwarz and Young's inequalities and use (22) along with the projection errors (19) and the trace inequality to obtain

$$\begin{aligned}
& \sum_{n=1}^{M-1} \sum_{i=1}^4 \Phi_i \\
& \leq \frac{1}{2} \theta_0 \kappa_{\mathbf{u}} \Delta t \sum_{n=1}^{M-1} \|D_t \xi_{\mathbf{u}}^{n+1}\|_{\mathcal{V}}^2 + \frac{1}{6} (c_0 - 3\alpha_m) \theta_0 \Delta t \sum_{n=1}^{M-1} \|D_t \xi_p^{n+1}\|_0^2 \\
& + \frac{1}{6} (C_d - 3\alpha_m \theta_0) \Delta t \sum_{n=1}^{M-1} \|D_t \xi_\theta^{n+1}\|_0^2 + C \Delta t \sum_{n=1}^{M-1} \left(\|D_t \chi_{\mathbf{u}}^{n+1}\|_{\mathcal{V}}^2 + \|D_t \chi_p^{n+1}\|_0^2 \right. \\
& \quad \left. + \|D_t \chi_\theta^{n+1}\|_0^2 \right) \\
& \leq \frac{1}{2} \theta_0 \kappa_{\mathbf{u}} \Delta t \sum_{n=1}^{M-1} \|D_t \xi_{\mathbf{u}}^{n+1}\|_{\mathcal{V}}^2 + \frac{1}{6} (c_0 - 3\alpha_m) \theta_0 \Delta t \sum_{n=1}^{M-1} \|D_t \xi_p^{n+1}\|_0^2 \\
& + \frac{1}{6} (C_d - 3\alpha_m \theta_0) \Delta t \sum_{n=1}^{M-1} \|D_t \xi_\theta^{n+1}\|_0^2 + Ch^2 \left(\|\mathbf{u}_t\|_{L^2(0,T; H^2(\Omega))}^2 \right. \\
& \quad \left. + \|p_t\|_{L^2(0,T; H^1(\Omega))}^2 + \|\theta_t\|_{L^2(0,T; H^1(\Omega))}^2 \right).
\end{aligned}$$

We similarly bound the next two terms. But, in this case, we use (21c) and that

$$\|D_t \mathbf{u}^{n+1} - \mathbf{u}_t^{n+1}\|_{\mathcal{V}}^2 = \|\boldsymbol{\epsilon}(D_t \mathbf{u}^{n+1} - \mathbf{u}_t^{n+1})\|_0^2 + \beta^{\mathbf{u}} \|h_e^{-\frac{1}{2}}(D_t \mathbf{u}^{n+1} - \mathbf{u}_t^{n+1})\|_{0,\partial\Omega}^2$$

due to the continuity of \mathbf{u} and \mathbf{u}_t across the interior edges (faces). As a result, we have

$$\begin{aligned}
& \sum_{n=1}^{M-1} \sum_{i=5}^6 \Phi_i \\
& \leq \frac{1}{6} (c_0 - 3\alpha_m) \theta_0 \Delta t \sum_{n=0}^{M-1} \|D_t \xi_p^{n+1}\|_0^2 + \frac{1}{6} (C_d - 3\alpha_m \theta_0) \Delta t \sum_{n=1}^{M-1} \|D_t \xi_\theta^{n+1}\|_0^2 \\
& + C \Delta t \|D_t \mathbf{u}^{n+1} - \mathbf{u}_t^{n+1}\|_{\mathcal{V}}^2 \\
& \leq \frac{1}{6} (c_0 - 3\alpha_m) \theta_0 \Delta t \sum_{n=0}^{M-1} \|D_t \xi_p^{n+1}\|_0^2 + \frac{1}{6} (C_d - 3\alpha_m \theta_0) \Delta t \sum_{n=1}^{M-1} \|D_t \xi_\theta^{n+1}\|_0^2 \\
& + C(\Delta t)^2 \left(\|\mathbf{u}_{tt}\|_{L^2(0,T; H^1(\Omega))}^2 + \frac{1}{h} \|\mathbf{u}_{tt}\|_{L^2(0,T; L^2(\partial\Omega))}^2 \right).
\end{aligned}$$

Once again, we bound the rest of the terms in the same manner as before.

$$\sum_{n=1}^{M-1} \sum_{i=7}^{14} \Phi_i$$

$$\begin{aligned}
&\leq \frac{1}{6}(C_d - 3\alpha_m\theta_0)\Delta t \sum_{n=1}^{M-1} \|D_t\xi_\theta^{n+1}\|_0^2 + \frac{1}{6}(C_d - 3\alpha_m\theta_0)\Delta t \sum_{n=1}^{M-1} \|D_t\xi_\theta^{n+1}\|_0^2 \\
&\quad + C \left(\|D_t\chi_p^{n+1}\|_0^2 + \|D_t\chi_\theta^{n+1}\|_0^2 + \|D_tp^{n+1} - p_t^{n+1}\|_0^2 + \|D_t\theta^{n+1} - \theta_t^{n+1}\|_0^2 \right) \\
&\leq \frac{1}{6}(c_0 - 3\alpha_m)\theta_0\Delta t \sum_{n=0}^{M-1} \|D_t\xi_p^{n+1}\|_0^2 + \frac{1}{6}(C_d - 3\alpha_m\theta_0)\Delta t \sum_{n=0}^{M-1} \|D_t\xi_\theta^{n+1}\|_0^2 \\
&\quad + C \left[h^2 \left(\|p_t\|_{L^2(0,T; H^1(\Omega))}^2 + \|\theta_t\|_{L^2(0,T; H^1(\Omega))}^2 \right) \right. \\
&\quad \left. + (\Delta t)^2 \left(\|p_{tt}\|_{L^2(0,T; L^2(\Omega))}^2 + \|\theta_{tt}\|_{L^2(0,T; L^2(\Omega))}^2 \right) \right].
\end{aligned}$$

Now, using the bound for the left-hand side in (31) and collecting the above bounds for the terms on the right-hand side, then combining with (27), we arrive at

$$\begin{aligned}
&\frac{1}{2}\theta_0\kappa_{\mathbf{u}}\Delta t \sum_{n=1}^{M-1} \|D_t\xi_{\mathbf{u}}^{n+1}\|_{\mathcal{V}}^2 + \frac{1}{2}\theta_0\kappa_p\|\xi_p^M\|_{\mathcal{W}}^2 + \frac{\kappa_\theta}{2}\|\xi_\theta^M\|_{\mathcal{W}}^2 \\
&\quad + \frac{\Delta t}{2} \sum_{n=1}^{M-1} (c_0 - 3\alpha_m)\theta_0 \|D_t\xi_p^{n+1}\|_0^2 + \frac{\Delta t}{2} \sum_{n=1}^{M-1} (C_d - 3\alpha_m\theta_0) \|D_t\xi_\theta^{n+1}\|_0^2 \\
&\leq C \left[h^2 \left(\|p^0\|_1^2 + \|\theta^0\|_1^2 + \|\mathbf{u}_t\|_{L^2(0,T; H^2(\Omega))}^2 + \|p_t\|_{L^2(0,T; H^1(\Omega))}^2 \right. \right. \\
&\quad \left. \left. + \|\theta_t\|_{L^2(0,T; H^1(\Omega))}^2 \right) + (\Delta t)^2 \left(\|\mathbf{u}_{tt}\|_{L^2(0,T; H^1(\Omega))}^2 + \frac{1}{h} \|\mathbf{u}_{tt}\|_{L^2(0,T; L^2(\partial\Omega))}^2 \right. \right. \\
&\quad \left. \left. + \|p_{tt}\|_{L^2(0,T; L^2(\Omega))}^2 + \|\theta_{tt}\|_{L^2(0,T; L^2(\Omega))}^2 \right) \right].
\end{aligned}$$

Note that all coefficients on the LHS are positive. Since this inequality holds for any arbitrary integer M between 2 and N , the discrete Gronwall lemma yields the desired error estimate (29). \square

Lemma 5.9 *Assume the conditions in (26) and that the penalty parameters $\beta^{\mathbf{u}}, \beta^p$, and β^θ are large enough. Also, assume that $\Delta t = \mathcal{O}(h) \ll 1$. Then, we have the following auxiliary error estimate:*

$$\begin{aligned}
&\Delta t \sum_{n=0}^N \left(\|\xi_p^n\|_{\mathcal{W}}^2 + \|\xi_\theta^n\|_{\mathcal{W}}^2 \right) + \max_{0 \leq n \leq N} \|\xi_{\mathbf{u}}^n\|_{\mathcal{V}}^2 + \max_{0 \leq n \leq N} \|\xi_p^n\|_0^2 + \max_{0 \leq n \leq N} \|\xi_\theta^n\|_0^2 \\
&\leq C \left[h^2 \left(\|p^0\|_1^2 + \|\theta^0\|_1^2 + \|\mathbf{u}_t\|_{L^2(0,T; H^2(\Omega))}^2 + \|p_t\|_{L^2(0,T; H^1(\Omega))}^2 \right. \right. \\
&\quad \left. \left. + \|\theta_t\|_{L^2(0,T; H^1(\Omega))}^2 \right) + (\Delta t)^2 \left(\|\mathbf{u}_{tt}\|_{L^2(0,T; H^1(\Omega))}^2 + \|\mathbf{u}_{tt}\|_{L^2(0,T; L^2(\partial\Omega))}^2 \right. \right. \\
&\quad \left. \left. + \|p_{tt}\|_{L^2(0,T; L^2(\Omega))}^2 + \|\theta_{tt}\|_{L^2(0,T; L^2(\Omega))}^2 \right) \right]. \tag{32}
\end{aligned}$$

Proof Take $\mathbf{v} = \theta_0\Delta t D_t\xi_{\mathbf{u}}^{n+1}$, $w = \theta_0\Delta t\xi_p^{n+1}$, and $s = \Delta t\xi_\theta^{n+1}$ in (24) and add the three equations and take summation over time from $n = 1$ to $M - 1$ for an integer $2 \leq M \leq N$ to obtain

$$\sum_{n=1}^{M-1} \left(\theta_0 \mathbf{a}_h^{\mathbf{u}}(\xi_{\mathbf{u}}^{n+1}, \xi_{\mathbf{u}}^{n+1} - \xi_{\mathbf{u}}^n) + \theta_0 \Delta t \mathbf{a}_h^p(\xi_p^{n+1}, \xi_p^{n+1}) + \Delta t \mathbf{a}_h^\theta(\xi_\theta^{n+1}, \xi_\theta^{n+1}) \right)$$

$$\begin{aligned}
& + \sum_{n=1}^{M-1} \left(c_0 \theta_0 (\xi_p^{n+1} - \xi_p^n, \xi_p^{n+1})_{\mathcal{T}_h} + C_d (\xi_\theta^{n+1} - \xi_\theta^n, \xi_\theta^{n+1})_{\mathcal{T}_h} \right) \\
& - 3\alpha_m \theta_0 \Delta t \sum_{n=1}^{M-1} \left((D_t \xi_\theta^{n+1}, \xi_p^{n+1})_{\mathcal{T}_h} + (D_t \xi_p^{n+1}, \xi_\theta^{n+1})_{\mathcal{T}_h} \right) \\
& = \sum_{n=1}^{M-1} \left[\alpha \theta_0 \Delta t \mathbf{b}_h (D_t \xi_{\mathbf{u}}^{n+1}, \chi_p^{n+1}) + 3\alpha_T K_{dr} \theta_0 \Delta t \mathbf{b}_h (D_t \xi_{\mathbf{u}}^{n+1}, \chi_\theta^{n+1}) \right. \\
& - \alpha \theta_0 \Delta t \mathbf{b}_h (D_t \chi_{\mathbf{u}}^{n+1}, \xi_p^{n+1}) - 3\alpha_T K_{dr} \theta_0 \Delta t \mathbf{b}_h (D_t \chi_{\mathbf{u}}^{n+1}, \xi_\theta^{n+1}) \\
& + \alpha \theta_0 \Delta t \mathbf{b}_h (D_t \mathbf{u}^{n+1} - \mathbf{u}_t^{n+1}, \xi_p^{n+1}) + 3\alpha_T K_{dr} \theta_0 \Delta t \mathbf{b}_h (D_t \mathbf{u}^{n+1} - \mathbf{u}_t^{n+1}, \xi_\theta^{n+1}) \\
& - c_0 \theta_0 \Delta t (D_t \chi_p^{n+1}, \xi_p^{n+1})_{\mathcal{T}_h} + 3\alpha_m \theta_0 \Delta t (D_t \chi_p^{n+1}, \xi_\theta^{n+1})_{\mathcal{T}_h} \\
& + 3\alpha_m \theta_0 \Delta t (D_t \chi_\theta^{n+1}, \xi_p^{n+1})_{\mathcal{T}_h} - C_d \theta_0 \Delta t (D_t \chi_\theta^{n+1}, \xi_p^{n+1})_{\mathcal{T}_h} \\
& + c_0 \theta_0 \Delta t (D_t p_t^{n+1} - p_t^{n+1}, \xi_p^{n+1})_{\mathcal{T}_h} - 3\alpha_m \theta_0 \Delta t (D_t p_t^{n+1} - p_t^{n+1}, \xi_\theta^{n+1})_{\mathcal{T}_h} \\
& \left. + C_d \Delta t (D_t \theta_t^{n+1} - \theta_t^{n+1}, \xi_\theta^{n+1})_{\mathcal{T}_h} - 3\alpha_m \theta_0 \Delta t (D_t \theta_t^{n+1} - \theta_t^{n+1}, \xi_p^{n+1})_{\mathcal{T}_h} \right] \\
& := \sum_{i=1}^{14} \mathcal{T}_i. \tag{33}
\end{aligned}$$

We can bound the left-hand side (LHS) of (33) from below, similarly to what we did to obtain (31). However, we use the following form of summation by parts to deal with the last term:

$$\begin{aligned}
& \sum_{n=1}^{M-1} (\phi^{n+1} - \phi^n) \psi^{n+1} + \sum_{n=1}^{M-1} \phi^{n+1} (\psi^{n+1} - \psi^n) \\
& = \phi^M \psi^M - \phi^1 \psi^1 + \sum_{n=1}^{M-1} (\phi^{n+1} - \phi^n) (\psi^{n+1} - \psi^n).
\end{aligned}$$

Then,

LHS

$$\begin{aligned}
& \geq \frac{1}{2} \theta_0 (\kappa_{\mathbf{u}} \|\xi_{\mathbf{u}}^M\|_{\mathcal{V}}^2 - C_{a_{\mathbf{u}}} \|\xi_{\mathbf{u}}^1\|_{\mathcal{V}}^2) + \Delta t \sum_{n=1}^{M-1} \left(\theta_0 \kappa_p \|\xi_p^{n+1}\|_{\mathcal{W}}^2 + \kappa_\theta \|\xi_\theta^{n+1}\|_{\mathcal{W}}^2 \right) \\
& + \frac{1}{2} c_0 \theta_0 (\|\xi_p^M\|_0^2 - C_{a_p} \|\xi_p^1\|_0^2) + \frac{1}{2} C_d (\|\xi_\theta^M\|_0^2 - C_{a_\theta} \|\xi_\theta^1\|_0^2) \\
& - 3\alpha_m \theta_0 (\xi_p^M, \xi_\theta^M)_{\mathcal{T}_h} + 3\alpha_m \theta_0 (\xi_p^1, \xi_\theta^1)_{\mathcal{T}_h} - 3\alpha_m \theta_0 (\Delta t)^2 \sum_{n=1}^{M-1} (D_t \xi_p^{n+1}, D_t \xi_\theta^{n+1})_{\mathcal{T}_h} \\
& \geq \frac{1}{2} \theta_0 (\kappa_{\mathbf{u}} \|\xi_{\mathbf{u}}^M\|_{\mathcal{V}}^2 - C_{a_{\mathbf{u}}} \|\xi_{\mathbf{u}}^1\|_{\mathcal{V}}^2) + \Delta t \sum_{n=1}^{M-1} \left(\theta_0 \kappa_p \|\xi_p^{n+1}\|_{\mathcal{W}}^2 + \kappa_\theta \|\xi_\theta^{n+1}\|_{\mathcal{W}}^2 \right) \\
& + \frac{1}{2} c_0 \theta_0 (\|\xi_p^M\|_0^2 - C_{a_p} \|\xi_p^1\|_0^2) + \frac{1}{2} C_d (\|\xi_\theta^M\|_0^2 - C_{a_\theta} \|\xi_\theta^1\|_0^2) \\
& - \frac{3\alpha_m \theta_0}{2} \left(\|\xi_p^M\|_0^2 + \|\xi_\theta^M\|_0^2 + \|\xi_p^1\|_0^2 + \|\xi_\theta^1\|_0^2 \right) \\
& - \frac{3}{2} \alpha_m \theta_0 (\Delta t)^2 \sum_{n=1}^{M-1} \left(\|D_t \xi_p^{n+1}\|_0^2 + \|D_t \xi_\theta^{n+1}\|_0^2 \right)
\end{aligned}$$

$$\begin{aligned}
&\geq \frac{1}{2}\theta_0\kappa_{\mathbf{u}}\|\xi_{\mathbf{u}}^M\|_{\mathcal{V}}^2 + \Delta t \sum_{n=1}^{M-1} \left(\theta_0\kappa_p\|\xi_p^{n+1}\|_{\mathcal{W}}^2 + \kappa_{\theta}\|\xi_{\theta}^{n+1}\|_{\mathcal{W}}^2 \right) \\
&\quad + \frac{1}{2}(c_0 - 3\alpha_m)\theta_0\|\xi_p^M\|_0^2 + \frac{1}{2}(C_d - 3\alpha_m\theta_0)\|\xi_{\theta}^M\|_0^2 \\
&\quad - \frac{1}{2}\theta_0C_{a_{\mathbf{u}}}\|\xi_{\mathbf{u}}^1\|_{\mathcal{V}}^2 - \frac{1}{2}(c_0C_{a_p} + 3\alpha_m)\theta_0\|\xi_p^1\|_0^2 - \frac{1}{2}(C_dC_{a_{\theta}} + 3\alpha_m\theta_0)\|\xi_{\theta}^1\|_0^2 \\
&\quad - \frac{3}{2}\alpha_m\theta_0(\Delta t)^2 \sum_{n=1}^{M-1} \left(\|D_t\xi_p^{n+1}\|_0^2 + \|D_t\xi_{\theta}^{n+1}\|_0^2 \right).
\end{aligned}$$

As this lower-bound of the LHS is bounded above by the right-hand side (RHS) of (33), we can obtain

$$\begin{aligned}
&\frac{1}{2} \left(\theta_0\kappa_{\mathbf{u}}\|\xi_{\mathbf{u}}^M\|_{\mathcal{V}}^2 + (c_0 - 3\alpha_m)\theta_0\|\xi_p^M\|_0^2 + (C_d - 3\alpha_m\theta_0)\|\xi_{\theta}^M\|_0^2 \right) \\
&\quad + \Delta t \sum_{n=1}^{M-1} \left(\theta_0\kappa_p\|\xi_p^{n+1}\|_{\mathcal{W}}^2 + \kappa_{\theta}\|\xi_{\theta}^{n+1}\|_{\mathcal{W}}^2 \right) \\
&\leq RHS + C \left[\|\xi_{\mathbf{u}}^1\|_{\mathcal{V}}^2 + \|\xi_p^1\|_0^2 + \|\xi_{\theta}^1\|_0^2 + (\Delta t)^2 \sum_{n=1}^{M-1} \left(\|D_t\xi_p^{n+1}\|_0^2 + \|D_t\xi_{\theta}^{n+1}\|_0^2 \right) \right]. \tag{34}
\end{aligned}$$

To complete the analysis, we turn to bound the RHS. First, rewrite \mathcal{T}_1 using summation by parts and bound it using the continuity of \mathbf{b}_h , the Cauchy-Schwarz and Young's inequalities, and appropriate Taylor expansions and projection error estimate as follows:

$$\begin{aligned}
\mathcal{T}_1 &= \alpha\theta_0 \sum_{n=1}^{M-1} \mathbf{b}_h(\xi_{\mathbf{u}}^{n+1} - \xi_{\mathbf{u}}^n, \chi_p^{n+1}) \\
&= \alpha\theta_0 \left(\mathbf{b}_h(\xi_{\mathbf{u}}^M, \chi_p^M) - \mathbf{b}_h(\xi_{\mathbf{u}}^1, \chi_p^1) - \Delta t \sum_{n=1}^{M-1} \mathbf{b}_h(\xi_{\mathbf{u}}^n, D_t\chi_p^{n+1}) \right) \\
&\leq \frac{1}{8}\theta_0\kappa_{\mathbf{u}}\|\xi_{\mathbf{u}}^M\|_{\mathcal{V}}^2 + C \left[\|\xi_{\mathbf{u}}^1\|_{\mathcal{V}}^2 + \|\chi_p^M\|_0^2 + \|\chi_p^1\|_0^2 + \Delta t \sum_{n=1}^{M-1} \left(\|\xi_{\mathbf{u}}^n\|_{\mathcal{V}}^2 + \|D_t\chi_p^{n+1}\|_0^2 \right) \right].
\end{aligned}$$

Similarly,

$$\mathcal{T}_2 \leq \frac{1}{8}\theta_0\kappa_{\mathbf{u}}\|\xi_{\mathbf{u}}^M\|_{\mathcal{V}}^2 + C \left[\|\xi_{\mathbf{u}}^1\|_{\mathcal{V}}^2 + \|\chi_{\theta}^M\|_0^2 + \|\chi_{\theta}^1\|_0^2 + \Delta t \sum_{n=1}^{M-1} \left(\|\xi_{\mathbf{u}}^n\|_{\mathcal{V}}^2 + \|D_t\chi_{\theta}^{n+1}\|_0^2 \right) \right].$$

The rest of the terms, $\mathcal{T}_3, \dots, \mathcal{T}_{14}$, can be bounded in the same manner as in the proof of Lemma 5.8. This will lead us to the following upper-bound of RHS:

RHS

$$\begin{aligned}
&\leq \frac{1}{4}\theta_0\kappa_{\mathbf{u}}\|\xi_{\mathbf{u}}^M\|_{\mathcal{V}}^2 + \frac{\Delta t}{2} \sum_{n=1}^{M-1} \left(\theta_0\kappa_p\|\xi_p^{n+1}\|_{\mathcal{W}}^2 + \kappa_{\theta}\|\xi_{\theta}^{n+1}\|_{\mathcal{W}}^2 \right) \\
&\quad + C \left[\Delta t \sum_{n=1}^{M-1} \left(\|\xi_p^{n+1}\|_0^2 + \|\xi_{\theta}^{n+1}\|_0^2 \right) + \|\xi_{\mathbf{u}}^1\|_{\mathcal{V}}^2 + \|\chi_p^M\|_0^2 + \|\chi_p^1\|_0^2 + \|\chi_{\theta}^M\|_0^2 \right. \\
&\quad \left. + \|\chi_{\theta}^1\|_0^2 + \Delta t \sum_{n=1}^{M-1} \left(\|D_t\chi_{\mathbf{u}}^{n+1}\|_0^2 + \|D_t\chi_p^{n+1}\|_0^2 + \|D_t\chi_{\theta}^{n+1}\|_0^2 \right) \right]
\end{aligned}$$

$$\begin{aligned}
& + \Delta t \sum_{n=1}^{M-1} \left(\|D_t \mathbf{u}^{n+1} - \mathbf{u}_t^{n+1}\|_0^2 + \|D_t p^{n+1} - p_t^{n+1}\|_0^2 + \|D_t \theta^{n+1} - \theta_t^{n+1}\|_0^2 \right) \\
& \leq \frac{1}{4} \theta_0 \kappa_{\mathbf{u}} \|\xi_{\mathbf{u}}^M\|_{\mathcal{V}}^2 + \frac{\Delta t}{2} \sum_{n=1}^{M-1} \left(\theta_0 \kappa_p \|\xi_p^{n+1}\|_{\mathcal{W}}^2 + \kappa_{\theta} \|\xi_{\theta}^{n+1}\|_{\mathcal{W}}^2 \right) \\
& + C \left[\Delta t \sum_{n=1}^{M-1} \left(\|\xi_p^{n+1}\|_0^2 + \|\xi_{\theta}^{n+1}\|_0^2 \right) + \|\xi_{\mathbf{u}}^1\|_{\mathcal{V}}^2 + h^2 \left(\|p^0\|_1^2 + \|\theta^0\|_1^2 \right. \right. \\
& \quad \left. \left. + \|\mathbf{u}_t\|_{L^2(0,T; H^1(\Omega))}^2 + \|p_t\|_{L^2(0,T; H^1(\Omega))}^2 + \|\theta_t\|_{L^2(0,T; H^1(\Omega))}^2 \right) \right. \\
& \quad \left. + (\Delta t)^2 \left(\|\mathbf{u}_{tt}\|_{L^2(0,T; L^2(\Omega))}^2 + \|p_{tt}\|_{L^2(0,T; L^2(\Omega))}^2 + \|\theta_{tt}\|_{L^2(0,T; L^2(\Omega))}^2 \right) \right].
\end{aligned}$$

Now, use this upper-bound and error estimates for the auxiliary errors at time t^1 in (27) and those for the discrete time derivatives in (29) to bound the right-hand side of (34). Finally, applying the discrete Gronwall lemma, we arrive at the desired error estimate (32). \square

6 Numerical Experiments

This section presents a set of numerical experiments aimed at validating the theoretical results presented in Section 5 and demonstrating the effectiveness and robustness of the proposed EG method. The computations are performed using deal.II, a finite element library [23], on quadrilateral meshes.

6.1 Example 1. Optimal convergence for smooth solutions

To verify the optimal convergence rate of the proposed method as proven in Theorem 5.1, we evaluate the method's performance on smooth solutions. The spatial domain is $\Omega = (0, 1)^2$, the final time is $T = 0.1$, and the following manufactured analytical solution is used:

$$\mathbf{u} = [\sin(\pi x t) \cos(\pi y t), \cos(\pi x t) \sin(\pi y t)], \quad p = \cos(t + x - y), \quad \theta = \sin(t + x - y),$$

from which the right-hand side functions \mathbf{f} , g , and h are obtained. The physical parameters are chosen to be simple numbers: $\alpha = \lambda = \mu = c_0 = C_d = 1$,

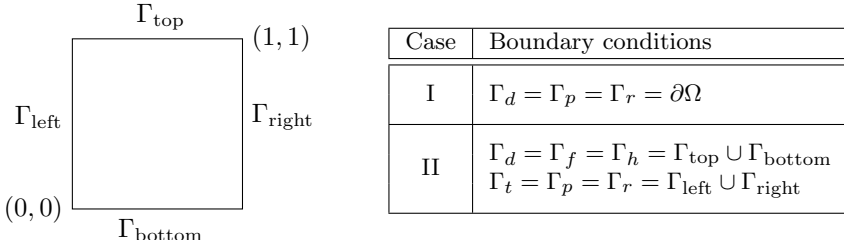


Fig. 1: Example 1: Boundary labels (left) and boundary conditions for two test cases (right).

$\alpha_T = 0.3$, $\alpha_m = 0.001$, $K_{dr} = (3\lambda + 2\mu)/3$, $\theta_0 = 1$, and $\mathbf{K} = \mathbf{D} = \mathbf{I}$, where \mathbf{I} is the 2×2 identity matrix. The penalty parameters are chosen as $\beta^u = \beta^p = \beta^\theta = 1000$.

As for boundary conditions, we consider two different combinations of boundary conditions. For case I, we impose pure Dirichlet boundary conditions for all three variables directly found from the exact solution. For case II, we use mixed boundary conditions, where we impose Neumann boundary condition for \mathbf{u} and Dirichlet boundary conditions for p and θ on the left and right sides, whereas we impose Dirichlet boundary condition for \mathbf{u} and Neumann boundary conditions for p and θ on the top and bottom sides. These boundary conditions for the two cases are summarized in Figure 1.

We solved the EG method and measured errors on five uniform meshes, starting with the initial mesh and timestep sizes of $h = 0.25$ and $\Delta t = 0.01$, halving them in each refinement cycle. The errors were measured in $\|\mathbf{u} - \mathbf{u}_h\|_{L^\infty(0,T; H^1(\mathcal{T}_h))}$, $\|p - p_h\|_{L^2(0,T; H^1(\mathcal{T}_h))}$, and $\|\theta - \theta_h\|_{L^2(0,T; H^1(\mathcal{T}_h))}$ norms, respectively. The convergence results are summarized in Figure 2, illustrating the expected optimal convergence rates for both cases.

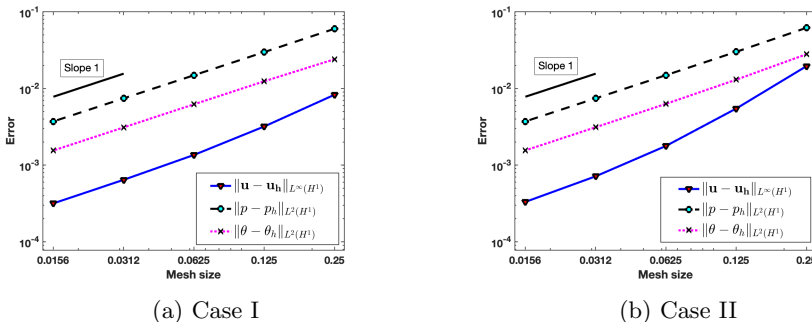


Fig. 2: Example 1: Convergence results.

6.2 Example 2. Solution with a large λ

In this example, we test our EG method against a solution with a large λ value. The error constant in our error estimates (16) depends on the Lamé constant λ ; hence the performance of our method may not be as good when λ is large. In this case, we can extend the EG method (7) by slightly modifying the bilinear form \mathbf{a}_h^u and the linear functional \mathbf{g}_h^u as follows. On a triangular mesh, we simply add an additional penalty term $\lambda^2 \gamma^u h_e \langle [\nabla \cdot \mathbf{w}], [\nabla \cdot \mathbf{v}] \rangle_{\mathcal{E}_h^I}$ to the bilinear form \mathbf{a}_h^u . On the other hand, it requires more modification on a quadrilateral mesh, where, in addition to a new penalty term, we also use the

reduced integration for the divergence operator in both $\mathbf{a}_h^{\mathbf{u}}$ and $\mathbf{g}_h^{\mathbf{u}}$:

$$\begin{aligned} \mathbf{a}_h^{\mathbf{u}}(\mathbf{w}, \mathbf{v}) := & 2\mu(\boldsymbol{\epsilon}(\mathbf{w}), \boldsymbol{\epsilon}(\mathbf{v}))_{\mathcal{T}_h} + \lambda(\mathcal{P}_0 \nabla \cdot \mathbf{w}, \mathcal{P}_0 \nabla \cdot \mathbf{v})_{\mathcal{T}_h} \\ & + \langle \{(2\mu\boldsymbol{\epsilon}(\mathbf{w}) + \lambda \mathcal{P}_0 \nabla \cdot \mathbf{w})\mathbf{n}_e\}, [\mathbf{v}]\rangle_{\mathcal{E}_h^I \cup \Gamma_d} - \langle [\mathbf{w}], \{(2\mu\boldsymbol{\epsilon}(\mathbf{v}) + \lambda \mathcal{P}_0 \nabla \cdot \mathbf{v})\mathbf{n}_e\}\rangle_{\mathcal{E}_h^I \cup \Gamma_d} \\ & + \beta^{\mathbf{u}} \langle h_e^{-1} [\mathbf{w}], [\mathbf{v}]\rangle_{e \in \mathcal{E}_h^I \cup \Gamma_d} + \lambda^2 \gamma^{\mathbf{u}} h_e \langle [\mathcal{P}_0 \nabla \cdot \mathbf{w}], [\mathcal{P}_0 \nabla \cdot \mathbf{v}]\rangle_{\mathcal{E}_h^I} \end{aligned} \quad (35a)$$

and

$$\begin{aligned} \mathbf{g}_h^{\mathbf{u}}(t; \mathbf{v}) := & (\mathbf{f}(t), \mathbf{v})_{\mathcal{T}_h} + \langle \mathbf{t}_N(t), \mathbf{v} \rangle_{\Gamma_t} - \langle \mathbf{u}_D(t), (2\mu\boldsymbol{\epsilon}(\mathbf{v}) + \lambda \mathcal{P}_0 \nabla \cdot \mathbf{v})\mathbf{n} \rangle_{\Gamma_d} \\ & + \beta^{\mathbf{u}} \langle h_e^{-1} \mathbf{u}_D(t), \mathbf{v} \rangle_{\Gamma_d}, \end{aligned} \quad (35b)$$

where \mathcal{P}_0 is the local L^2 -projection onto the piecewise constant space \mathbb{P}_0^{DG} . No error estimates have yet been proved independently of λ for these modified methods. However, the following numerical test shows promising results for the case of a large λ .

Here, our manufactured solution is

$$\begin{aligned} \mathbf{u} = & \left[\sin(\pi xt) \sin(\pi yt) + \frac{1}{\lambda} xt, \cos(\pi xt) \cos(\pi yt) + \frac{1}{\lambda} yt \right], \\ p = & \cos(t + x - y), \text{ and } \theta = \sin(t + x - y) \end{aligned}$$

in a computational domain $\Omega \times \mathbb{I} = (0, 1)^2 \times (0, 0.1]$. The functions \mathbf{f}, g , and h are obtained from the exact solution. For boundary conditions, we employ pure Dirichlet boundary conditions for all variables. Note that $\nabla \cdot \mathbf{u} = 2t/\lambda \rightarrow 0$ as $\lambda \rightarrow \infty$ at any time t . We used the following physical parameters: $\alpha = \mu = c_0 = C_d = 1$, $\alpha_T = 10^{-6}$, $\alpha_m = 10^{-8}$, $\lambda = 10^6$, $K_{dr} = (3\lambda + 2\mu)/3$, $\theta_0 = 1$, and $\mathbf{K} = \mathbf{D} = \mathbf{I}$. As before, we used $\beta^{\mathbf{u}} = \beta^p = \beta^\theta = 1000$. But, we also used an additional penalty parameter $\gamma^{\mathbf{u}} = 10^{-5}$ in (35). With the above physical and penalty parameters, we performed the same convergence study as in Example 1. The convergence behaviors of the EG method are illustrated in Figure 3, where we see the optimal convergence rates for all three variables even when λ is very large. In other words, no Poisson locking is shown.

6.3 Example 3. Injection and production of the fluid

This example considers a more realistic scenario in, for example, geothermal reservoir simulations, where we simulate injection-production processes in the domain. Our spatial domain is $\Omega = (0, 1)^2$ with injection and production wells situated at $(0.25, 0.5)$ and $(0.75, 0.5)$, respectively. The injection and production functions for the pressure and temperature are defined as

$$g(x, y) = g_c e^{(-1000(x-x_1)^2 - 1000(y-y_1)^2)} - g_c e^{(-1000(x-x_2)^2 - 1000(y-y_2)^2)}, \quad (36a)$$

$$h(x, y) = h_c e^{(-1000(x-x_1)^2 - 1000(y-y_1)^2)} - h_c e^{(-1000(x-x_2)^2 - 1000(y-y_2)^2)} \quad (36b)$$

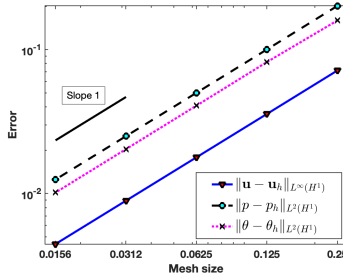


Fig. 3: Example 2: Convergence results with a large λ value.

with $g_c = 1$, $h_c = 10$, $(x_1, y_1) = (0.25, 0.5)$ and $(x_2, y_2) = (0.75, 0.5)$, while the external force function $\mathbf{f} = \mathbf{0}$. Regarding the boundary conditions, we impose the homogeneous Dirichlet boundary condition for \mathbf{u} ($\mathbf{u}_D = \mathbf{0}$) and the homogeneous Neumann boundary conditions for both p and θ ($q_N = s_N = 0$) on the entire boundary $\partial\Omega$. The initial conditions are set to be $\mathbf{u}^0 = \mathbf{0}$, $p^0 = 0$, and $\theta^0 = 100$. Additionally, the following physical parameters are used: $\lambda = 10$, $\mu = 1$, $\alpha_T = 10^{-4}$, $\alpha_m = 10^{-6}$, $\alpha = 1$, $c_0 = 10^{-5}$, $C_d = 10.0$, $\theta_0 = 100$, $\mathbf{K} = 10^{-4}\mathbf{I}$, and $\mathbf{D} = \mathbf{I}$. The penalty parameters were set to $\beta^u = \beta^p = \beta^\theta = 1000$. Finally, we used the mesh and time step sizes $h = 0.02$, and $\Delta t = 0.001$, and the final time is $T = 1$.

The simulation results at the final time are shown in Figures 4-6. First, Figure 4 (a) presents the vector fields of the displacement, where we clearly observe the expansion and compression of the medium due to injection and production, respectively. Figure 4 (b) provides another perspective, illustrating the deformation of the mesh by the projected displacement. Figures 5 and 6 illustrate the pressure and temperature profiles. We note that the temperature solution is more diffusive than the pressure due to the larger conductivity than the permeability value.

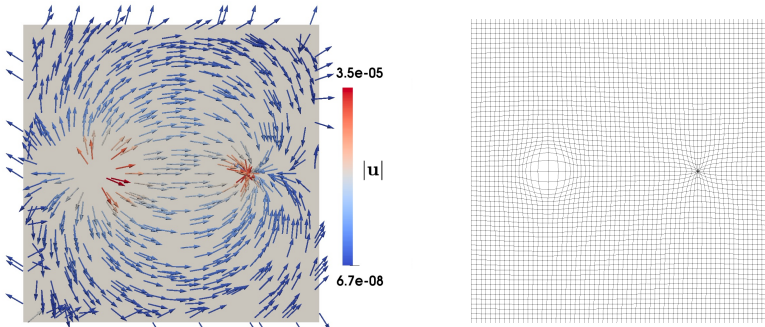


Fig. 4: Example 3: Displacement, \mathbf{u} , at $T = 1$ illustrated by vector fields (left) and a deformed mesh (right).

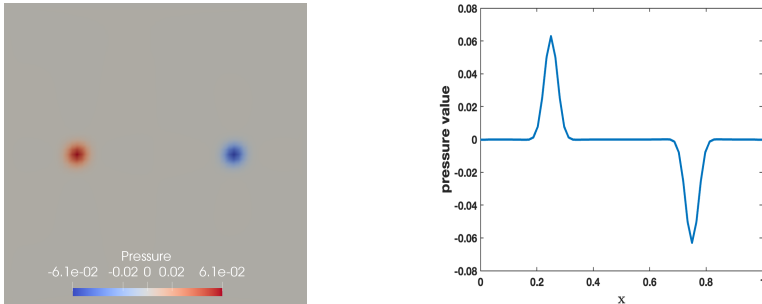


Fig. 5: Example 3: Pressure, p , at $T = 1$ (left) and a cross-section across the line $y = 0.5$ (right).

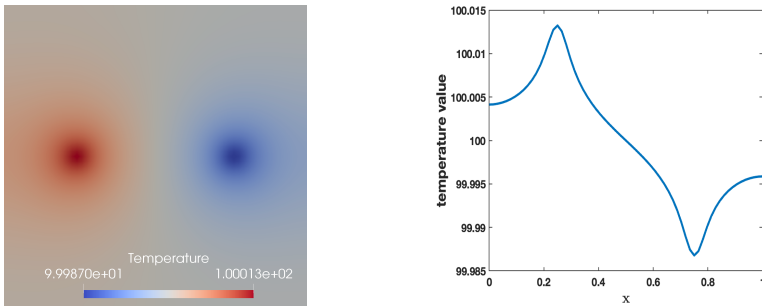


Fig. 6: Example 3: Temperature, θ , at $T = 1$ (left) and a cross-section across the line $y = 0.5$ (right).

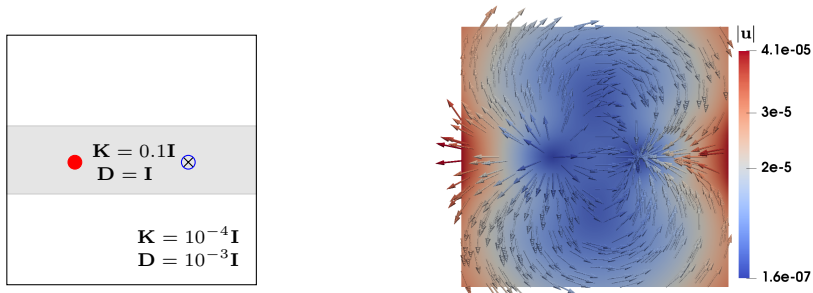
6.4 Example 4. A solution in a heterogeneous medium and local conservation property

In this final example, we consider a heterogeneous domain $\Omega = (-0.5, 0.5)^2$ with a larger permeability and conductivity zone in the center of the domain than the rest of the domain, as shown in Figure 7 (left). Specifically, the permeability and conductivity values are $\mathbf{K} = 10^{-1}\mathbf{I}$ and $\mathbf{D} = \mathbf{I}$ in the middle layer and $\mathbf{K} = 10^{-4}\mathbf{I}$ and $\mathbf{D} = 10^{-3}\mathbf{I}$ in other layers. As in Example 3, we simulate injection-production processes realized by the source and sink functions defined as in (36) with $g_c = h_c = 10^{-2}$, $(x_1, y_1) = (-0.25, 0)$, and $(x_2, y_2) = (0.25, 0)$. Also, the external force function is $\mathbf{f} = \mathbf{0}$. We imposed the homogeneous Neumann boundary conditions for all three variables on the entire boundary $\partial\Omega$. The initial conditions are set to be $\mathbf{u}^0 = \mathbf{0}$, $p^0 = 0$, and $\theta^0 = 1$.

The rest of the data are as follows: $\lambda = 1$, $\mu = 1$, $c_0 = 10^{-2}$, $C_d = 1$, $\alpha_T = 10^{-4}$, $\alpha_m = 10^{-6}$, $\alpha = 1$, and $\theta_0 = 1$. This time, we used the following penalty parameters: $\beta^u = \beta^p = \beta^\theta = 100$. We also used mesh and time step sizes of $h = 0.01$ and $\Delta t = 0.1$ with $T = 20$.

Figure 7 depicts vector fields of the displacement, \mathbf{u} , while Figure 8 depicts the pressure and temperature solutions at the final time. These figures show that all three solutions have no oscillations or non-physical phenomena near the material interfaces.

As one of our primary interests is the local conservation properties of our EG method, we measured the residuals in the discrete local mass and energy conservation equations, (13a) and (13b). It is well-known that the classical CG method lacks these properties. Hence, for comparison's sake, we solved the same problem using the bilinear CG method and measured the residuals in the continuous local mass and energy conservation equations, (12a) and (12b). More specifically, we measured the absolute difference between the left- and right-hand sides of these conservation equations on each mesh element $K \in \mathcal{T}_h$. The residuals of the local mass conservation equations, (13a) and (12a), are



(a) Example 4: domain

(b) Vector fields of \mathbf{u}

Fig. 7: Example 4: Heterogeneous medium with injection and production wells (left) and the vector fields of \mathbf{u} at $T = 20$ (right).

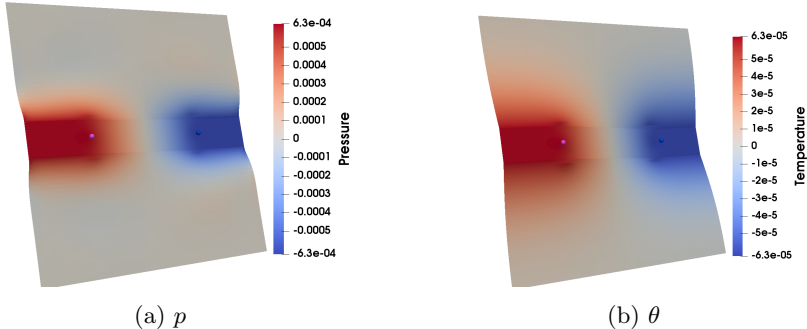


Fig. 8: Example 4: (a) Pressure and (b) temperature profiles at $T = 20$.

denoted by R_p , and those of the local energy conservation equations, (13b) and (12b), are denoted by R_θ . Note that R_p and R_θ are piecewise constant functions on the mesh \mathcal{T}_h . Figures 9 and 10 show the residuals at the final time of the simulation. The figures show that the EG method produces several-order magnitude smaller residuals than the CG method for both the mass and energy conservation equations. Also, it appears that while the larger residuals in the CG method are concentrated near the wells, those in the EG method are mostly near the domain boundary in the middle layer. We also monitored the maximum residuals over time, that is, $\|R_\theta\|_{L^\infty(\Omega)}$ and $\|R_p\|_{L^\infty(\Omega)}$ for $0 < t \leq T$, for mass and energy conservation equations. These results are depicted in Figure 11, where we observe that the maximum residual values for mass and energy conservation in the EG method decrease over time as the system approaches its equilibrium state. However, the maximum residual values in the CG method remain nearly constant during the entire simulation period.

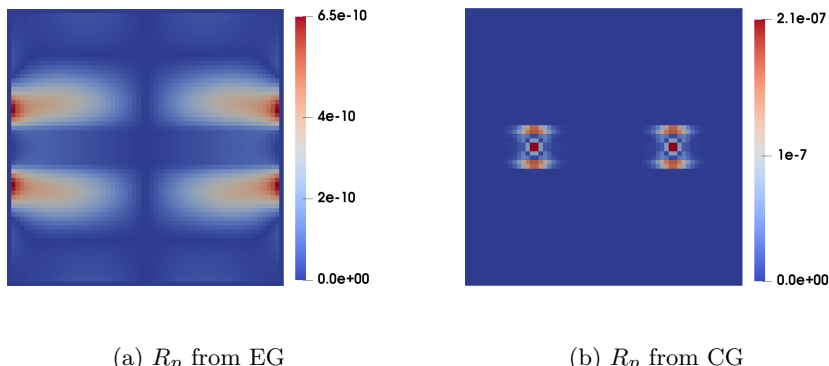


Fig. 9: Example 4. Residual, R_p , in the local mass conservation equations at the final time.

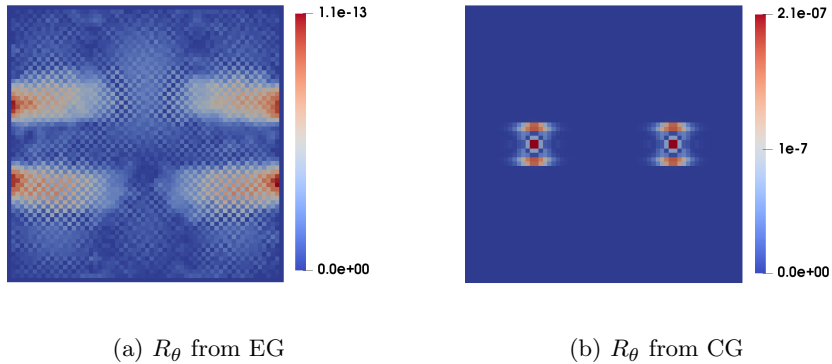


Fig. 10: Example 4: Residual, R_θ , in the local energy conservation equations at the final time.

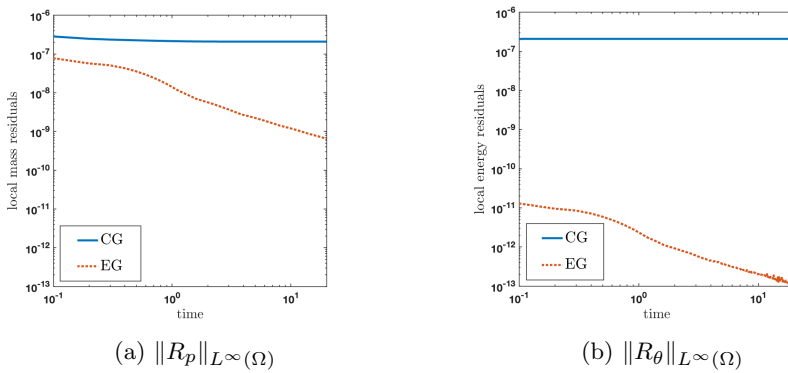


Fig. 11: Example 4. Maximum local mass and energy residuals over time.

Acknowledgments. The work of S.-Y. Yi was partially supported by the U.S. National Science Foundation under Grant DMS-2208426 and by the U.S. Department of Energy, Office of Science, Energy Earthshots Initiatives under Award Number DE-SC-0024703. The work of S. Lee was partially supported by the U.S. National Science Foundation Grant DMS-2208402 and by the U.S. Department of Energy, Office of Science, Energy Earthshots Initiatives under Award Number DE-SC-0024703.

References

- [1] Biot, M.: Thermoelasticity and irreversible thermodynamics. *Journal of Applied Physics* **27**(3), 240–253 (1956)
- [2] Biot, M.: General theory of three-dimensional consolidation. *J. Appl. Phys.* **12**(2), 155–164 (1941)
- [3] Pandey, S., Vishal, V., Chaudhuri, A.: Geothermal reservoir modeling in a coupled thermo-hydro-mechanical-chemical approach: a review. *Earth-Science Reviews* **185**, 1157–1169 (2018)
- [4] Settgast, R.R., Fu, P., Walsh, S.D., White, J.A., Annavarapu, C., Ryerson, F.J.: A fully coupled method for massively parallel simulation of hydraulically driven fractures in 3-dimensions. *Int. J. Numer. Anal. Methods. Geomech.* **41**(5), 627–653 (2017)
- [5] Williams, M.D., Vermeul, V.R., Reimus, P., Newell, D., Watson, T.B.: Development of models to simulate tracer behavior in enhanced geothermal systems. Technical report, Pacific Northwest National Lab.(PNNL), Richland, WA (United States) (2010)
- [6] Pruess, K.: The tough codes a family of simulation tools for multiphase flow and transport processes in permeable media. *Vadose zone journal* **3**(3), 738–746 (2004)
- [7] Zyvoloski, G.: Finite element methods for geothermal reservoir simulation. *Int. J. Numer. Anal. Methods. Geomech.* **7**(1), 75–86 (1983)
- [8] Al-Khoury, R., Bonnier, P., Brinkgreve, R.: Efficient finite element formulation for geothermal heating systems. part I: Steady state. *Int. J. Numer. Methods Eng.* **63**(7), 988–1013 (2005)
- [9] Zhang, J., Rui, H.: Galerkin method for the fully coupled quasi-static thermo-poroelastic problem. *Computers & Mathematics with Applications* **118**, 95–109 (2022)
- [10] Xia, Y., Podgorney, R., Huang, H.: Assessment of a hybrid continuous/discontinuous Galerkin finite element code for geothermal reservoir

simulations. *Rock Mechanics and Rock Engineering* **50**(3), 719–732 (2017)

- [11] Einstein, H., Vecchiarelli, A.: Further development and application of geofrac-flow to a geothermal reservoir. Technical report, Massachusetts Inst. of Technology (MIT), Cambridge, MA (United States) (2014)
- [12] Brun, M.K., Ahmed, E., Nordbotten, J.M., Radu, F.A.: Well-posedness of the fully coupled quasi-static thermo-poroelastic equations with nonlinear convective transport. *Journal of Mathematical Analysis and Applications* **471**(1), 239–266 (2019)
- [13] Sun, S., Liu, J.: A locally conservative finite element method based on piecewise constant enrichment of the continuous Galerkin method. *SIAM J. Sci. Comput.* **31**(4), 2528–2548 (2009)
- [14] Lee, S., Lee, Y.-J., Wheeler, M.F.: A locally conservative enriched Galerkin approximation and efficient solver for elliptic and parabolic problems. *SIAM J. Sci. Comput.* **38**(3), 1404–1429 (2016)
- [15] Lee, S., Wheeler, M.F.: Adaptive enriched Galerkin methods for miscible displacement problems with entropy residual stabilization. *J. Comput. Phys.* **331**, 19–37 (2017)
- [16] Lee, S., Wheeler, M.F.: Enriched Galerkin methods for two-phase flow in porous media with capillary pressure. *J. Comput. Phys.* **367**, 65–86 (2018)
- [17] Choo, J., Lee, S.: Enriched Galerkin finite elements for coupled poromechanics with local mass conservation. *Comput. Methods Appl. Mech. Engng.* **341**, 311–332 (2018)
- [18] Yi, S.-Y., Lee, S., Zikatanov, L.: Locking-free enriched Galerkin method for linear elasticity. *SIAM J. Numer. Anal.* **60**(1), 52–75 (2022)
- [19] Yi, S.-Y., Hu, X., Lee, S., Adler, J.H.: An enriched Galerkin method for the Stokes equations. *Computers & Mathematics with Applications* **120**, 115–131 (2022)
- [20] Lee, S., Yi, S.-Y.: Locking-free and locally-conservative enriched Galerkin method for poroelasticity. *Journal of Scientific Computing* (2023)
- [21] Zimmerman, R.: Coupling in poroelasticity and thermoelasticity. *International Journal of Rock Mechanics and Mining Sciences* **37**(1-2), 79–87 (2000)
- [22] Cacace, M., Jacquay, A.B.: Flexible parallel implicit modelling of coupled

thermal–hydraulic–mechanical processes in fractured rocks. *Solid Earth* **8**(5), 921–941 (2017)

- [23] Arndt, D., Bangerth, W., Davydov, D., Heister, T., Heltai, L., Kronbichler, M., Maier, M., Pelteret, J.-P., Turcksin, B., Wells, D.: The **deal.II** library, version 8.5. *Journal of Numerical Mathematics* (2017)